Source Partitioning of H_2O and CO_2 Fluxes Based on High Frequency Eddy Covariance Data: a Comparison between Study Sites

Anne Klosterhalfen[1], Alexander Graf[1], Nicolas Brüggemann[1], Clemens Drüe[2], Odilia Esser[1], María Pat
González Dugo[3], Günther Heinemann[2], Cor M.J. Jacobs[4], Matthias Mauder[5], Arnold F. Moene[6],
Patrizia Ney[1], Thomas Pütz[1], Corinna Rebmann[7], Mario Ramos Rodríguez[3], Todd M. Scanlon[8], Marius
Schmidt[1], Rainer Steinbrecher[5], Christoph K. Thomas[9], Veronika Valler[1], Matthias J. Zeeman[5], Harry
Vereecken[1]

[1]Agrosphere Institute, IBG-3, Forschungszentrum Jülich GmbH, 52425 Jülich, Germany
[2]Department of Environmental Meteorology, University of Trier, 54296 Trier, Germany
[3]IFAPA - Consejería de Agricultura, Pesca y Desarrollo Rural, Centro Alameda del Obispo, 14080 Córdoba, Spain
[4]Wageningen Environmental Research, Wageningen University and Research, 6708 PB Wageningen, the Netherlands
[5]Institute of Meteorology and Climate Research, IMK-IFU, Karlsruhe Institute of Technology (KIT), 82467 Garmisch-
Partenkirchen, Germany
[6]Meteorology and Air Quality Group, Wageningen University and Research, 6708 PB Wageningen, the Netherlands
[7]Department Computational Hydrosystems, Helmholtz Centre for Environmental Research (UFZ), 04318 Leipzig, Germany
[8]Department of Environmental Sciences, University of Virginia, Charlottesville, VA 22904, United States
[9]Micrometeorology Group, University of Bayreuth, 95447 Bayreuth, Germany

Correspondence to: Anne Klosterhalfen (a.klosterhalfen@fz-juelich.de)

Abstract. For an assessment of the roles of soil and vegetation in the climate system, a further understanding of the flux components of H_2O and CO_2 (e.g., transpiration, soil respiration) and their interaction with physical conditions and physiological functioning of plants and ecosystems is necessary. To obtain magnitudes of these flux components, we applied the source partitioning approaches after Scanlon and Kustas (2010; SK10) and after Thomas et al. (2008; TH08) to high frequency eddy covariance measurements of twelve study sites covering different ecosystems (croplands, grasslands, and forests) in different climatic regions. Both partitioning methods are based on higher-order statistics of the H_2O and CO_2 fluctuations, but proceed differently to estimate transpiration, evaporation, net primary production, and soil respiration. We compared and evaluated the partitioning results obtained with SK10 and TH08 including slight modifications of both approaches. Further, we analyzed the interrelations between the performance of the partitioning methods, turbulence characteristics, and site characteristics (such as plant cover type, canopy height, canopy density, and measurement height). We were able to identify characteristics of a data set that are prerequisite for adequate performance of the partitioning methods.

SK10 had the tendency to overestimate and TH08 to underestimate soil flux components. For both methods, the partitioning of CO_2 fluxes was less robust than of H_2O fluxes. Results derived with SK10 showed relatively large dependencies on estimated water use efficiency (WUE) at the leaf level, which is a required input. Measurements of outgoing longwave

radiation used for the estimation of foliage temperature (used in WUE) could slightly increase the quality of the partitioning results. A modification of the TH08 approach, by applying a cluster analysis for the conditional sampling of respiration/evaporation events, performed satisfactorily, but did not result in significant advantages compared to the original method versions developed by Thomas et al. (2008). The performance of each partitioning approach was dependent on

5 meteorological conditions, plant development, canopy height, canopy density, and measurement height. Foremost, the performance of SK10 correlated negatively with the ratio between measurement height and canopy height. The performance of TH08 was more dependent on canopy height and leaf area index. In general, all site characteristics which increase dissimilarities between scalars appeared to enhance partitioning performance for SK10 and TH08.

1 Introduction

10 The eddy covariance (EC) method is a micrometeorological technique commonly used to measure the energy, water vapor, and carbon dioxide exchange between biosphere and atmosphere across a large range of scales in time and space (Baldocchi et al., 2001; Reichstein et al., 2012). The measurements help to understand the temporal and spatial variations of these fluxes at the land-atmosphere interface. However, the EC method quantifies only net fluxes of water vapor, i.e. evapotranspiration (ET), and the net ecosystem exchange of CO_2 (NEE). Thus, for a better assessment of the role of soil and vegetation in the

15 climate system, a further understanding of the flux components of H_2O and CO_2 and their interaction with physical conditions and physiological functioning of plants and ecosystems is necessary (Baldocchi et al., 2001). To obtain magnitudes of transpiration, evaporation, photosynthesis, and respiration by soil and vegetation, certain measurements with additional instrumentation independent of the EC technique can be conducted. Alternatively or additionally, so-called source partitioning approaches can be applied to the net fluxes obtained with the EC method. For instance, with the notion that

20 during night no CO_2 is assimilated by plants (and hence, observed NEE equals respiration), respiratory fluxes are often estimated based on semi-empirical models describing the relationship between a physical driver (e.g., temperature) and respiration (Lloyd and Taylor, 1994; Reichstein et al., 2005, 2012). To estimate soil surface fluxes of both H_2O and CO_2 directly from high frequency EC data without assumptions on such drivers, two distinct partitioning approaches were developed by Scanlon and coauthors (Scanlon and Sahu, 2008; Scanlon and Kustas, 2010), and Thomas et al. (2008). Both

25 approaches rely on the assumption that the presence of multiple sources and sinks in and below the canopy will lead to decorrelation of the high frequency scalar concentrations measured by the EC method above the canopy. This decorrelation contains information about the strength of these sinks and sources, which can be quantified by applying the flux-variance similarity theory or conditional sampling strategies. The scalar-scalar-correlations of H_2O and CO_2 are however not only influenced by the sink-source distribution, but also by height (atmospheric surface layer, roughness sublayer), surface

30 heterogeneity (Williams et al., 2007), canopy density, and coherent structures (Edburg et al., 2012; Huang et al., 2013).
The source partitioning approach after Scanlon and Sahu (2008) and Scanlon and Kustas (2010) has already been applied to data acquired above a corn field (eastern USA; Scanlon and Kustas, 2012), has been compared to an isotopic H_2O flux

partitioning method (Good et al., 2014) and to the Noah Land Surface Model (Wang et al., 2016) both for grasslands, and has been evaluated on a forest site on a decadal time scale (Sulman et al., 2016). Zeeman et al. (2013) further investigated the partitioning approach after Thomas et al. (2008) in association with coherent structures. To better assess these two approaches and their theoretical background, an intercomparison at a variety of study sites is necessary (Anderson et al., 2018).

The objective of this study is to compare and evaluate the source partitioning approaches after Scanlon and Kustas (2010) and after Thomas et al. (2008) by applying them to high frequency scalar measurements of various study sites in different ecosystems. In addition to testing slight modifications of both partitioning methods, conditions and characteristics of study sites are identified under which the methods perform best. Based on findings of the above-mentioned authors and a large eddy simulation (LES) study (Klosterhalfen et al., 2019), we hypothesize that the methods' performance is dependent on the canopy height (h_c), which should represent the vertical separation of sinks and sources of H_2O and CO_2 between canopy top and soil surface, on the canopy density (leaf area index LAI, or expressed as the ratio LAI h_c^{-1}), and on the ratio between measurement height (z) and h_c, respectively. All these factors affect the degree of mixing of the scalars detected by the EC sensors. With a high and sparse canopy and a low z h_c^{-1}, we hypothesize a larger dissimilarity between scalar fluctuations and a more precise partitioning result of both source partitioning approaches. To summarize, goals of this study are:

- The comparison and evaluation of the partitioning results obtained with the approaches after Scanlon and Kustas (2010) and after Thomas et al. (2008) for various ecosystems, and testing slight modifications of the approaches

- An analysis of the two approaches with respect to their dependence on their underlying assumptions

- The description of the interrelations between performance of the partitioning methods, turbulence characteristics, and site characteristics (such as canopy type, h_c, z h_c^{-1}, LAI, and LAI h_c^{-1})

- The identification of characteristics of a data set (i.e. of study site and period properties), which lead to a satisfactory performance of the partitioning methods, if such characteristics exist.

2 Material and Methods

2.1 Source Partitioning after Scanlon and Kustas (2010) - SK10

To estimate the contributions of transpiration (T), evaporation (E), photosynthesis as net primary production (NPP), and soil respiration ($R_{soil,}$ autotrophic and heterotrophic sources) to the measured net fluxes, Scanlon and Sahu (2008) and Scanlon and Kustas (2010) proposed a source partitioning method using high frequency time series from a typical EC station. This method (SK10 in the following) is based on the spatial separation and relative strength of sinks and sources of water vapor and CO_2 below the canopy (source of both water vapor and CO_2), in the canopy (source of water vapor and sink of CO_2 during daylight), and the atmosphere. Assuming that air from those sinks and sources is not yet perfectly mixed before reaching the EC sensors, partitioning is estimated based on the separate application of the flux-variance similarity theory to the stomatal and non-stomatal components of the scalars, as well as an estimation of canopy water use efficiency (WUE).

The slope of the relationship between water vapor fluctuations (q') and CO_2 fluctuations (c') originating from stomatal and non-stomatal processes usually differs from the WUE at the leaf level and the correlation between the two scalars ($\rho_{q'c'}$) usually deviates from -1 during daytime. This deviation of the slope of the q' versus c' relationship from WUE at leaf-level and the reduction of correlation are used to estimate the composition of the measured fluxes (Scanlon and Kustas, 2010; Scanlon and Sahu, 2008). For a detailed analytical description of SK10 see Scanlon and Albertson (2001), Scanlon and Sahu (2008), Scanlon and Kustas (2010, 2012), and Palatella et al. (2014). Furthermore, Skaggs et al. (2018) implemented SK10 in the open source Python 3 module Fluxpart. In the present study, SK10 was applied to high frequency EC data and the flux components were estimated using the implementation of SK10 as described by Klosterhalfen et al. (2019).

As mentioned before, the WUE at the leaf level has to be estimated for the application of SK10. WUE at the leaf level describes the relation between the amount of CO_2 uptake through stomata (photosynthesis) and the corresponding amount of H_2O loss (T). One way to derive WUE (without additional measurements at leaf-level) is to relate the difference in mean CO_2 concentration between air outside and inside the leaf to the difference in mean water vapor concentration between air outside and inside the leaf including a factor that accounts for the difference in diffusion rate between H_2O and CO_2 through the stomatal aperture (Campbell and Norman, 1998; Scanlon and Sahu, 2008). The mean H_2O and CO_2 concentrations just outside the leaf can be inferred from EC measurements by considering logarithmic mean concentration profiles implementing the Monin-Obukhov similarity theory (MOST; Scanlon and Kustas, 2010, 2012; Scanlon and Sahu, 2008). For the internal CO_2 concentration, a constant value of 270 or 130 ppm was presumed, typical for C_3 or C_4 plants, respectively (Campbell and Norman, 1998; Špunda et al., 2005; Williams et al., 1996; Xue et al., 2004). Values for the internal water vapor concentration were estimated based on 100% relative humidity at foliage temperature. Measurements of foliage temperature were not available at the study sites, so for the source partitioning foliage temperature was set equal to measured air temperature (WUE$_{meanT}$; Scanlon and Sahu, 2008). Additionally, to investigate the sensitivity of WUE, foliage temperature was also derived by means of measured outgoing longwave radiation (WUE$_{OLR}$; with a surface emissivity of 0.98), or calculated similar to the external concentrations by considering a mean profile based on MOST (WUE$_{MOST}$). Thus, three different approaches of SK10 with differing inputs for WUE were applied to all study sites.

2.2 Source Partitioning after Thomas et al. (2008) - TH08

Thomas et al. (2008) presented a new method (TH08 in the following) to estimate daytime sub-canopy respiration of forests directly from EC raw data by conditional sampling. In an analogous way, evaporation can be quantified by exchanging c' with q' in the equations given by Thomas et al. (2008, equations 1-11, pages 1212-1215). The method assumes that occasionally air parcels moving upward (vertical wind fluctuations $w' > 0$) carry unaltered H_2O/CO_2 concentration combinations of the sub-canopy. Looking at the fluctuations q' and c', both normalized with the corresponding standard deviation, respiration/evaporation signals should occur within the part of the joint probability distribution where w', q' and c' are positive, i.e. in the first quadrant in the q'-c' plane (where $q' > 0$ and $c' > 0$). Additionally, Thomas et al. (2008) introduced a hyperbolic threshold criterion within quadrant 1, in order to only sample all data points above this hyperbola.

Thomas et al. (2008) found realistic respiration estimates with a hyperbolic threshold of 0.25, which was also applied here. Subsequently, daytime evaporation and respiration can be determined from the conditionally sampled w', q', and c' time series within quadrant 1 (Q1) or using the hyperbola threshold criterion (H). For the determination of the turbulent H_2O and CO_2 fluxes either the covariance between w' and the corresponding scalar (CV) can be used, or the relaxed eddy

5   accumulation (REA) technique (Businger and Oncley, 1990) using the coefficient β as described in equation 4, page 1213 and statements on page 1215 in Thomas et al. (2008). Hence, Thomas et al. (2008) applied four different approaches to quantify the respiration/evaporation events, combining the two conditional sampling criteria (Q1 or H) and the two calculation strategies (CV or REA technique).

For some averaging periods in our data, a potential respiration/evaporation 'cloud' was evident but did not occur

10   (completely) within quadrant 1 (Fig. 1). As a modification of the conditional sampling strategy and a more tolerant detection of respiration/evaporation events, a distribution-based cluster analysis was conducted (fifth approach, GMM). With the Gaussian Mixture Model (Canty, 2010) using the Expectation-Maximization Algorithm, two clusters were defined for each averaging period: the respiration/evaporation 'cloud' and all further points associated with T and photosynthesis independent of the sign of w'. Soil surface fluxes were calculated by CV from data in the respiration/evaporation 'cloud', where the

15   deviations from the averages of all sampled cluster data points (instead of all data points) were used for q' and c' (w' kept unchanged). Because the sampled respiration/evaporation 'cloud' by GMM would not always lie within quadrant 1 (often in quadrant 1 and 4, or in 1 and 2), and q' and/or c' of the defined 'cloud' could correlate negatively with w', the corresponding surface flux would often be negative (Fig. 1). If this was the case for H_2O and/or CO_2 soil fluxes, the corresponding flux was recalculated considering the deviations from the averages of all data points for w', q', and c', and only including data points

20   within quadrant 1 of the original q'-c' plane and with $w' > 0$. This recalculated flux represented only a minimal fraction of the corresponding flux component in the considered averaging period. Also, as a result of this procedure the number of data points could differ between H_2O and CO_2 for TH08 CV GMM depending on the calculation step used.

2.3 Study Sites and Data Processing

For the application and evaluation of the source partitioning methods, various study sites in a number of countries with

25   differing cover types, canopy densities (represented by LAI), and measurement heights were chosen (Table 1). Almost all study sites are part of the FLUXNET network (Baldocchi et al., 2001). Detailed site and measurement descriptions can be found in the listed references. Besides coniferous and deciduous forests with closed canopy cover, grasslands, and croplands, some sites represent special canopy types: in Forest_SC (for site abbreviations see Table 1) EC measurements have been conducted above a Mediterranean oak savanna (dehesa; Andreu et al., 2018); in Wüstebach an area of about 9 ha was

30   deforested in 2013 and so measurements were obtained above the still present spruce forest (Forest_WU) and the deforested area (Grass_WU) (Graf et al., 2014; Wiekenkamp et al., 2016), where grass, shrubs, and young deciduous trees have been regrowing swiftly; and in Forest_LA a coniferous forest has been regrowing gradually after a non-cleared windthrow in 2007 (Matiu et al., 2017). These three study sites represent the most heterogeneous landcover types in this study.

For each study site, measurements from days with a high-productive state of the vegetation and fair-weather conditions were selected to exclude factors interfering with the performance of the partitioning method. Time periods with precipitation events were excluded. Furthermore, the quality assessment scheme after Mauder et al. (2013) was applied to each data set and source partitioning was only conducted for time periods with the highest or intermediate quality flag levels assigned by this scheme. We only considered partitioning results of daytime data, because both methods require the presence of photosynthesis. Here, daytime was determined by calculating sunrise and sunset times by means of local time. Additionally, the TH08 method was only applied to time periods with a negative $\rho_{q'c'}$, and if less than 1% of the total data points in one half-hour time period were sampled as the respiration/evaporation 'event', the partitioning result was disregarded.

The high frequency H_2O and CO_2 time series of all study sites were pre-processed and prepared for the application of the source partitioning approaches as described by Klosterhalfen et al. (2019). For each study site, physically impossible values and spikes were excluded in the high frequency EC data of vertical wind, total H_2O and CO_2 concentrations. The time delay was corrected, missing raw data within a half-hour period were gap-filled by linear interpolation, and a planar-fit rotation was conducted, where the rotation matrix was calculated for only a maximum time period of two weeks. Further, the EC data was corrected for density fluctuations after Detto and Katul (2007). Then, the source partitioning approaches were applied to half-hourly time series of these pre-processed high frequency data, partitioning fractions (E/ET or R_{soil}/NEE, respectively) were calculated, and applied to the post-processed half-hourly EC data.

2.4 Evaluation of Source Partitioning Results

The evaluation of the source partitioning performance was conducted in multiple ways for the various study sites depending on data-availability. At some study sites, R_{soil} was measured additionally with closed-chamber measurements independently of the EC measurements. In Grass_RO and the cropland in Selhausen (Wheat_SE, Barley_SE, Intercrop_SE, SugarBeet_SE), continuous measurements of multiple longterm-chambers were available for the considered time periods (half-hourly at Selhausen and hourly interpolated to half-hourly at Grass_RO). In Maize_DI, Forest_WU, and Grass_WU, R_{soil} was measured with survey-chambers at several measurement points on one day during the considered time periods, so spatial and temporal averages for the hours in question could be calculated. For all study sites, soil evaporation (E_{soil}) was estimated as a fraction of measured ET based on Beer's law depending on LAI (E_{soil} = ET exp(-0.6 LAI); Campbell and Norman, 1998; Denmead et al., 1996). Thus, the root mean square error (RMSE) and the bias could be calculated between the partitioning results for E or R_{soil} and the estimated E_{soil} or chamber measurements, respectively. RMSE was sensitive to bias and outliers, and the distribution of errors was skewed. The positive outliers/errors (overestimations) were larger than negative errors (underestimations). An overestimation of the flux component magnitude may result in a larger RMSE than an underestimation. Therefore, we also calculated a version of the RMSE based on log-transformed data ($RMSE_{ln}$; data transformed with ln(x +1)) before computing differences between estimated and reference E or R_{soil}. Furthermore, one has to keep in mind that the measurements of R_{soil} and LAI can also contain errors and that E_{soil} is only a rough model approximation and can only give an order of magnitude to expect.

In addition, partitioned CO_2 fluxes were evaluated in reference to results of the established partitioning approach after Reichstein et al. (2005), if available; even though this approach targets other flux components (total ecosystem respiration TER and gross primary production GPP). For Forest_MMP and Forest_WA, results of this partitioning approach were not available, thus, we chose for these sites maximal margins for GPP and TER based on partitioning results of previous years and experience. For all sites, the estimated NPP and R_{soil} for every time step were classified as reasonable if their magnitudes were smaller than the determined GPP or TER, respectively. Since all data sets were from the main growing season and for weather conditions favorable to high respiration, we assumed that R_{soil} should additionally be larger than 1 µmol m^{-2} s^{-1}. In the following, NPP and R_{soil} estimates meeting these criteria ("hits in range") will be counted as HiR GPP (magnitude of NPP smaller than magnitude of GPP) and HiR TER (R_{soil} smaller than TER and larger than 1 µmol m^{-2} s^{-1}). We calculated the percent fraction of HiR GPP and HiR TER in relation to the count of time steps with valid partitioning solutions. Within this evaluation step two source partitioning approaches (approach after Reichstein et al., 2005 versus SK10 or TH08) were examined and compared including their different assumptions and uncertainties, and the results have to be handled with care. An evaluation of the estimated flux magnitudes was also possible for some study sites by means of prior publications.

2.5 Analysis of Source Partitioning Approaches

To compare the strengths and limitations of SK10 and TH08 and to gain a better insight in their functionality and dependencies on turbulence and site characteristics, a correlation analysis was conducted between HiR GPP or HiR TER and the variables z, h_c, $z\ h_c^{-1}$, LAI, or LAI h_c^{-1}. Here, we have chosen HiR GPP and HiR TER as the criteria of partitioning performance, because these could be calculated for all considered study sites, unlike the error metrics (RMSE, bias, etc.) regarding R_{soil}. Different subsets of sites were considered for the calculation of the correlations: all study sites, only forest sites, or only cropland and grassland sites.

SK10 was already thoroughly analyzed by means of synthetic high frequency data derived by LES (Klosterhalfen et al., 2019). To obtain a better understanding of the strengths and limitations of TH08, we constructed a conceptual model to generate simple, synthetic data sets of w', q', and c' (with sample sizes of N = 100) with different degrees of mixing between scalar sinks and sources from the soil, canopy, and boundary layer (Fig. 7, *upper panels*). We considered no mixing, complete mixing, and partial mixing between scalars originating from soil and canopy (with positive w'). For all three sets, mixing with scalars originating from the boundary layer (with negative w') was excluded. Averages of fluctuations were all specified as zero, and each scalar sink/source strength was determined such that the net H_2O flux equals to 1 mmol m^{-2} s^{-1} and the net CO_2 flux to -1 µmol m^{-2} s^{-1}. To each generated data point of w', q' and c' a random number, sampled from a standard normal distribution and rescaled to a standard deviation of 5% of the magnitude of the variable, was added to simulate additional sources of variance not related to the degree of mixing. TH08 was applied to these synthetic data sets and could be validated with the true known partitioning fractions

3 Results and Discussion

For each study site, the number of half-hourly time steps during daylight per considered time period is shown in Table A1 in the Appendix. Also, the fraction of daylight time steps of high-quality (HQ) data which were used in the application of SK10 and TH08 are shown, where for SK10 only a good or intermediate quality flag (after Mauder et al., 2013) and no

5 precipitation were required, and for TH08 additionally a negative $\rho_{q'c'}$. Furthermore, the fraction of these HQ-time steps, for which partitioning solutions were found, is shown for each method version. Thus, from the original data, only a part remained for the partitioning, and for only a part of the remaining data a partitioning result could be obtained.

3.1 Evaluation of Source Partitioning Results

3.1.1 Flux Components Magnitudes

10 In the following, figures are shown for some selected sites, which were deemed most representative for all study sites, and/or for some selected method versions of SK10 and TH08, which usually exhibited the best partitioning performance. In Fig. 2 the source partitioning results for H_2O and CO_2 fluxes for Forest_LO are shown in half-hourly time steps as an example. The partitioning results for all sites and all method versions are shown in the Supplementary material, including E_{soil} estimations based on Beer's law, chamber measurements of R_{soil}, and/or partitioning results after Reichstein et al. (2005), depending on

15 data-availability. Figures 3 and 4 show the mean diurnal variation of H_2O and CO_2 fluxes and their components. Figure 3 shows data from one site (Forest_WA) and all method versions, whereas Fig. 4 shows results for all study sites and just two method versions: SK10 with WUE_{OLR} and TH08 with REA H. In Fig. 5 the total averages of the flux components over the available time periods are shown. The top panel compares all method versions for a single site (Forest_MMP) whereas the lower two panels compare all sites for two method versions (SK10 with WUE_{OLR} and TH08 with REA H). For the

20 calculation of these mean diurnal variations as well as the total averages, large spikes in the estimated flux components (deviation from the mean by more than ten times of the standard deviation) were excluded. Figure 6 shows the error quantities, $RMSE_{ln}$ and bias relative to R_{soil} chamber measurements, HiR GPP, HiR TER, and E_{soil} estimation, for each site and method version. In all figures, timestamps are in local time.

In general, the partitioned CO_2 fluxes showed a higher variability and more spikes than the partitioned H_2O fluxes for all

25 sites (e.g., at Forest_HH, Fig. S2 in Supplementary material). Furthermore, SK10 and TH08 gave differing results for each study site and performed disparately between method versions. In Fig. 2-5, it is apparent that TH08 mostly resulted in lower magnitudes of the flux components originating from the soil surface or sub-canopy than SK10. The source partitioning results of Forest_LO (Fig. 2, 4, 5) were an exception to this rule. For this study site, the partitioning fractions of SK10 and TH08 were very similar and thus suggest a low uncertainty of the results. For the other study sites, larger discrepancies were

30 observed between SK10 and TH08. Furthermore, the partitioning fractions E/ET and NPP/NEE varied much less between sites for TH08 than for SK10 (Fig. 5). Good et al. (2015) determined a global estimate for T/ET of 0.65 and Schlesinger and Jasechko (2014) an estimate of 0.61. Li et al. (2019) deduced mean annual partitioning fractions of 0.75, 0.62, and 0.56 for

evergreen coniferous forests, croplands, and grasslands, respectively. Our derived partitioning fractions had approximately the same magnitudes or assigned a larger fraction to transpiration, most likely due to the seasons chosen. We could not observe a clear difference in partitioning fractions between ecosystem types as Li et al. (2019).

For a number of our sites, information on component fluxes is available from literature. For Forest_LO in 1997, Dolman et al. (2002) reported a peak respiration measurement of 12 $\mu mol\ m^{-2}\ s^{-1}$, Falge et al. (2002) a seasonal maximum GPP of -24 $\mu mol\ m^{-2}\ s^{-1}$ and seasonal maximum TER of 5.3 $\mu mol\ m^{-2}\ s^{-1}$, and chamber measurements in June 2003 revealed a maximum soil respiration rate of 17.3 $\mu mol\ m^{-2}\ s^{-1}$. Our partitioning results for Forest_LO based on SK10, TH08, and the approach after Reichstein et al. (2005) laid within the range of these reported flux magnitudes (Fig. 2, S1 in Supplementary material). For Forest_WA, SK10-derived partitioning fractions, with T/ET > 0.5 and NPP/NEE > 2, were relatively large. On 8 July 2016, however, the CO_2 flux components were smaller, with NPP/NEE < 1.4 and R_{soil} < 10 $\mu mol\ m^{-2}\ s^{-1}$ (Fig. S4 in Supplementary material). On this day no significant differences in weather conditions or scalar statistics were apparent in contrast to the other days. For Forest_MMP, Thomas et al. (2009) derived a T/ET ratio of 50% from sap flow measurements, which agrees well with the partitioning results obtained with the SK10 approach (Fig. 5, Fig. S6 in Supplementary material). Results of the TH08 approach and estimated E_{soil} imply a relatively larger fraction of T. At Forest_SC, the results of the different source partitioning methods were impacted by water stress. For a very dry period in August 2016, both partitioning approaches were not applicable, because transpiration and photosynthesis almost ceased due to water stress, and the correlations between H_2O and CO_2 fluxes were almost always positive (not shown). In April 2017, partitioning results were obtained showing an increase in R_{soil} estimated with SK10 and a decrease in estimated E (Fig. S7 in Supplementary material). Spring 2017 was considered as relatively dry in this region, and the last precipitation event was five days before the respective time period, so that it can be assumed that water stress increased steadily in April 2017. No respiration/evaporation events were apparent in the *q'-c'* planes, which could be caused by the sub-canopy in the oak savanna, thus, TH08 probably underestimated soil fluxes substantially.

In Grass_RO the continuous chamber measurements of R_{soil} and TER estimated with the approach after Reichstein et al. (2005) did not agree well. TER decreased steadily over the seven days (this could also be observed for Grass_FE) and was mostly lower than measured R_{soil} (Fig. S8 in Supplementary material). In comparison to measured R_{soil}, SK10 still overestimated and TH08 underestimated R_{soil} fluxes. For Forest_WU and Grass_WU, TH08 yielded results matching comparatively well with the modeled estimate E_{soil} and the gap-filling approach after Reichstein et al. (2005) (Fig. S3, S9 in Supplementary material). As mentioned before, Grass_WU is a very heterogeneous site with regrowing vegetation of grasses, shrubs, and trees on dry and wet areas. Thus, the measured signals might display fluxes originating from different sinks and sources distributed horizontally rather than vertically. The present variety of plant types increased the uncertainty in the estimation of WUE. Usage of WUE_{OLR} improved the partitioning by SK10 significantly, but could not avoid overestimation of R_{soil} (in reference to chamber measurements and TER). For Forest_LA, we observed a behavior similar to Grass_WU (Fig. S5 in Supplementary material). Here, the forest is also regrowing, but spruce trees are already more abundant and larger.

For Maize_DI in 2007, Jans et al. (2010) reported a mean R_{soil} flux of 3.16 μmol m^{-2} s^{-1} and a peak R_{soil} of 23 μmol m^{-2} s^{-1}. R_{soil} estimates by SK10 were often as large as this peak, but the maximum observed by Jans et al. (2010) was triggered by precipitation, which does not apply in our case (Fig. S11 in Supplementary material). The partitioning results for the cropland in Selhausen (Wheat_SE, Barley_SE, Intercrop_SE, SugarBeet_SE) showed large differences between crops and were more robust for H_2O fluxes than CO_2 fluxes.

3.1.2 Error Metrics

Figure 6 shows the error metrics RMSE$_{ln}$ and bias relative to chamber measurements of R_{soil}, HiR GPP, HiR TER, and RMSE$_{ln}$ and bias relative to E_{soil} estimation, for each site and method version. A clear pattern in the performance of the source partitioning depending on method version or on study site characteristics could not be identified in the error metrics (Fig. 6). However, the following general statements can be made:

1) The RMSE in R_{soil} was usually larger for SK10 than for TH08 (not shown). Considering RMSE$_{ln}$ in R_{soil}, SK10 performed better at forest sites than TH08, and slightly worse at crop- and grasslands (Fig. 6a). The bias in R_{soil} was always positive for SK10 (except for Forest_WU) and often negative for TH08 (except for TH08 REA H; Fig. 6b); SK10 has the tendency to overestimate and TH08 to underestimate R_{soil} compared to respiration chamber measurements. The lowest RMSE, RMSE$_{ln}$, and bias were found for the SK10 method versions in Forest_WU and for TH08 in Forest_WU, Grass_WU, and SugarBeet_SE_09.

2) When using the gap-filling model after Reichstein et al. (2005) as a reference, high HiR GPP were relatively frequent for TH08, with a minimum of 66.7% for SugarBeet_SE_06, while HiR GPP for SK10 were considerably lower (Fig. 6c). For HiR TER, such a clear difference in performance could not be observed (Fig. 6d). While SK10 mostly overestimated TER, TH08 often estimated soil fluxes smaller than the minimum R_{soil} threshold of 1 μmol m^{-2} s^{-1}. TH08 REA H usually gave the best results for HiR TER and the worst for HiR GPP within the method versions of TH08. Also, the performance of SK10 improved for CO_2 in Maize_DI with increasing crop height and lower LAI (Fig. 4, 6).

3) The RMSE (not shown), RMSE$_{ln}$, and bias of E (in reference to E_{soil} estimated using Beer's law) were mostly similar or slightly larger for SK10 than for TH08 except for the low crop canopies, Forest_LO, Forest_MMP, and Forest_SC (Fig. 6e, f). These sites also had a relatively low LAI. The error metrics were low in Forest_WU and Grass_WU for SK10 and TH08. The worst performance regarding E could be found in Forest_HH for SK10, and in Forest_SC, Maize_DI_06, and Intercrop_SE for TH08. The bias indicated that SK10 underestimated E for all canopies with a LAI lower than 2.3 (Forest_LO, Forest_SC, Maize_DI_06, SugarBeet_SE_06, Intercrop_SE, the latter three have relatively short canopies). This could also be explained by the larger E_{soil} estimates based on Beer's law due to the smaller LAIs, thus preventing an overestimation by SK10.

To summarize, for TH08 the calculation of the fluxes via REA yielded larger fluxes than via CV (Fig. 2, 3, 5). Because averaging in the flux calculation is performed differently for CV and REA (i.e. equations 1, page 1212 and equation 8, page 1214 in Thomas et al., 2008), and fewer data points are sampled with the hyperbolic threshold than using data from the entire

Q1, the largest magnitudes were obtained by using REA with the hyperbolic threshold (REA H). In some time steps, no respiration/evaporation 'cloud' was apparent in the q'-c' plane, thus, the applied conditional sampling strategies were not as effective as intended, and an assessment of a correct sampling was not possible. Using GPP and TER estimated with the gap-filling model after Reichstein et al. (2005) as reference, components estimated by TH08 almost always were within this prescribed range (i.e. magnitude of NPP smaller than magnitude of GPP, and R_{soil} smaller than TER) because of their small resulting fluxes, whereby R_{soil} was often below the assumed minimum threshold of 1 μmol m^{-2} s^{-1}; thus, we assume these values to be underestimated (Fig. 6, S1-S13 in Supplementary material). Regarding the error metrics in Fig. 6, TH08 REA H, among all TH08 method versions, yielded the best result for the largest number of sites and error metrics. Partitioning results obtained by TH08 CV GMM were not systematically different from the other method versions, but showed no extreme spikes in the soil flux components.

The SK10 approach had the tendency to produce very high values of the soil flux components. Considering the diurnal dynamics and averages (Fig. 3-5), results of SK10 were satisfactory, but still relatively large. For most of the study sites, the magnitudes and variability in the half-hourly results of the soil flux components were decreased by using WUE_{MOST} or WUE_{OLR} instead of WUE_{meanT}. The differing WUE inputs had a larger effect on the CO_2 flux components than on H_2O. The magnitudes of the estimated leaf-level WUEs agreed well with magnitudes stated by Good et al. (2014), Linderson et al. (2012), and Sulman et al. (2016). Considering the error metrics in Fig. 6, SK10 with WUE_{OLR} very often gave the best results.

3.2 Analysis of Source Partitioning Approaches

3.2.1 Analysis by Means of Correlation Analysis

We studied the interrelations between partitioning performance (expressed in HiR GPP and HiR TER) and site characteristics such as canopy height h_c, LAI, canopy density (using LAI h_c^{-1} as proxy), measurement height z, and the position of the measurements relative to the roughness sublayer (using z h_c^{-1} as a proxy) by means of a correlation analysis (Tables 2, 3). Here, h_c represents the vertical separation of sinks and sources of passive scalars between canopy top and soil surface. For the chosen study sites, LAI correlated with h_c when considering a specific ecosystem type (forest, cropland, or grassland). Thus, LAI h_c^{-1} was also considered to distinguish between their impacts on partitioning performance. The ecosystem type "cropland" included only two different sites, Maize_DI and Selhausen (Wheat_SE, Barley_SE, Intercrop_SE, SugarBeet_SE), and thus only two different measurement heights z, but a total of nine data sets resulting from the considered time periods and various crops (Table 1). Therefore, the correlation coefficients with z including this ecosystem type have to be handled with care. All these site characteristics contain some information about the characteristics of the observed turbulence and also affect the degree of mixing of the scalars when they reach the EC sensor. Furthermore, we assume that with increasing LAI, LAI h_c^{-1} and z h_c^{-1}, and with decreasing h_c the dissimilarity between q' and c' decreases and EC measurements contain less information for the partitioning approaches (Edburg et al., 2012; Huang et al., 2013;

Williams et al., 2007). Results of Klosterhalfen et al. (2019) suggest a decreasing performance of SK10 with increasing $z\,h_c^{-1}$.

Correlation coefficients between partitioning performance and site characteristics were calculated for all sites together, for forests only, or for crop- and grasslands only, respectively (Tables 2, 3). For the SK10 method versions, the correlation coefficients showed similar relations between variables and partitioning results for both HiR GPP and HiR TER, because SK10 had the tendency to overestimate both NPP and R_{soil}. For the TH08 method versions, relations slightly differ between HiR GPP and HiR TER, because TH08 had the tendency to underestimate R_{soil} fluxes ($< 1\ \mu mol\ m^{-2}\ s^{-1}$), thus HiR TER were smaller than HiR GPP. For the forest sites, the correlations were relatively high between variables and partitioning performance, even though mostly not significantly different from zero.

The performance of all SK10 method versions correlated negatively with LAI h_c^{-1} and $z\,h_c^{-1}$, and positively with h_c and z, where the correlation with $z\,h_c^{-1}$ was often significant. The correlation coefficients regarding LAI, despite being also positive, were the smallest. Therefore, partitioning performance of SK10 was mostly enhanced with a sparse canopy and measurements obtained close to the canopy (close to or within roughness sublayer). For the TH08 method versions, LAI had larger effects on partitioning performance than for SK10 method versions, and h_c, $z\,h_c^{-1}$, and LAI h_c^{-1} had smaller effects. Correlation coefficients of LAI and LAI h_c^{-1} were mostly positive with a few exceptions (e.g., regarding HiR TER for crop- and grasslands). For the TH08 method versions, all site characteristics correlated positively with HiR GPP, except for $z\,h_c^{-1}$ considering all study sites. The correlations between site characteristics and HiR TER were weak while considering all study sites. For forest sites, HiR TER correlated negatively with LAI h_c^{-1} and $z\,h_c^{-1}$ and positively with h_c, LAI, and z. For crop- and grasslands, similar results were obtained, except the negative correlation between HiR TER and LAI. Also, the correlations with h_c and z increased in significance. Apparently, a dense canopy yielded too low sub-canopy fluxes derived by TH08, but more reasonable canopy fluxes.

The variable LAI mostly correlated positively with partitioning performance for TH08 method versions and very weak with partitioning performance for SK10 method versions, which contradicted our initial hypotheses. Also, the correlation between partitioning performance by TH08 and LAI h_c^{-1} at forest sites contradicted our assumption that a higher plant density would have a strong negative effect. Next to canopy density, LAI could also be connected to larger sinks and sources of canopy fluxes (T and photosynthesis) relative to soil surface fluxes due to larger biomass, and to the appearance and frequency of coherent structures. A dense canopy prevents frequent ejections of air parcels from the sub-canopy, but provokes higher scalar concentrations in such air parcels because of a longer accumulation under the canopy. Respiration/evaporation events could occur less frequently but be of higher magnitude. Also, small gaps in an otherwise dense canopy can play an important role regarding ejection events. Thus, how canopy density affects scalar-scalar-correlation measured above the canopy (and associated with that the partitioning performance), cannot be easily assessed. In this study, canopy density (LAI and LAI h_c^{-1}) and partitioning performance (especially regarding HiR TER) correlated negatively at crop- and grassland sites and mostly positively at the forest sites for TH08. Assuming gaps in the canopy can be more frequent in forests than in crop- or grasslands, these results support the above-mentioned aspects. Zeeman et al. (2013) found a clear connection between the

appearance of coherent structures and the detection of respiration/evaporation events following the TH08 approach, where the best results were obtained for an open canopy (Forest_MMP). They found a temporal separation of 10-20 s between sub-, mid-, and above-canopy measurements. In order to assess to what extent these effects play a role in the current data sets, an estimate of the (large-scale) heterogeneity and density of the vegetation at all study sites (gap fraction, canopy openness) would be necessary, which is beyond the scope of this paper.

3.2.2 Analysis by Means of a Conceptual Model

SK10 was already thoroughly analyzed by means of the synthetic high frequency data derived by LES (Klosterhalfen et al., 2019). In the present study, TH08 was applied to various synthetic w'-, q'-, and c'-data sets including soil, canopy, and boundary layer scalar sink/sources derived by a simple conceptual model as described above (Fig. 7, *top panel*). Defined by the conditional sampling concept, we hypothesized that TH08 would work perfectly with no mixing of the scalars from the three different origins, would not obtain any partitioning fractions in case of the complete mixing, and would underestimate the soil fluxes in case of partial mixing.

TH08 behaved as hypothesized except for TH08 REA H (see below; Fig. 7, *bottom panel*). For the partial mixing, a small difference in TH08-derived partitioning fractions (especially for H_2O) was observed between the sampling in Q1 and with H, because one data point was not sampled with the hyperbolic threshold, but was located within Q1. TH08 REA H did not yield any partitioning results in case of no or partial mixing. This is due to the different definitions of β in the application of REA with the sampling in Q1 or with H (Thomas et al., 2008, equation 4, page 1213 and statement on page 1215). β is an empirical constant and can be approximated by the ratio between the standard deviation of w' ($\sigma_{w'}$) and the difference between the mean vertical velocities in updrafts and downdrafts ($\overline{w_+} - \overline{w_-}$). For the conditional sampling approach within Q1, β is derived including all data points (disregarding the sign of q' or c'). For the approach including the hyperbolic threshold criterion, β is derived from w' data points which satisfy the hyperbolic threshold criterion for positive q' and c'. In case of our conceptual model for the partial mixing, no data point with negative w' satisfied this criterion, so without $\overline{w_-}$, β and a partitioning fraction could not be calculated. Figure 7 shows the partitioning fractions for TH08 REA H while applying β as calculated in TH08 REA Q1 (*non-filled markers*). TH08 CV GMM performed similar to the other method versions: it sampled the correct respiration/evaporation 'cloud' in case of no mixing and no 'cloud' in case of complete mixing. However, in case of the partial mixing all data points with $q' > 0$ were sampled by TH08 CV GMM, thus, considering also the fraction originating from the canopy. For the latter, the covariances applying the averages of q or c of the sampled cluster, and considering only data points with $w' > 0$, were negative for H_2O and CO_2 (not shown). Thus, E and R_{soil} were recalculated with the covariance taking the deviations of the average of q or c considering all data points, and including only data points with $w' > 0$, within quadrant 1, and within the sampled cluster. This way of correcting the sampling by GMM resulted in a similar partitioning fraction as the other method versions.

4 Summary and Conclusions

For all sites and all applied method versions, the partitioned CO_2 fluxes generally showed a higher variability and more spikes than the partitioned H_2O fluxes. Mean diurnal cycles averaged over each site's specific time period yielded satisfactory results. The partitioning approaches after Scanlon and Kustas (2010; SK10) and after Thomas et al. (2008; TH08) gave differing results and performed disparately between method versions. TH08 mostly resulted in lower magnitudes of the flux components originating from the soil surface than SK10. In addition, TH08 had the tendency to underestimate these flux components in reference to soil respiration flux measurements and estimates of E_{soil} based on Beer's law. SK10 usually had the tendency to overestimate soil flux components and yielded larger error metrics (RMSE and bias). The RMSE depends on the bias and the error distribution was asymmetric. The positive errors (overestimations) were larger than negative errors (underestimations). Decreasing the weight of outliers by log-transforming R_{soil} data from chamber observations and partitioning estimations revealed a lower $RMSE_{ln}$ for SK10 at forest sites than for TH08.

SK10 was used with a variety of estimates of WUE. Estimating input WUE using foliage temperature derived from the observed outgoing longwave radiation often improved the partitioning performance. For TH08, various options were tested regarding the conditional sampling and flux calculation. Applying a Gaussian Mixture Model for the conditional sampling approach in TH08 did not improve partitioning performance significantly, because obtaining a positive and correct flux estimation was difficult for data points outside quadrant 1 in the q'-c' plane. For TH08, conditional sampling including a hyperbolic threshold and calculating flux components based on the relaxed eddy accumulation technique yielded the best partitioning results.

The dependencies of the partitioning performance on turbulence and site characteristics were analyzed based on a correlation analysis and the application of TH08 to synthetic, conceptual data sets of scalar fluctuations. Foremost, the performance of SK10 was improved for sparse canopies and especially with a low ratio between measurement height and canopy height. The performance of TH08 was more dependent on canopy height and leaf area index. Partitioning performance of TH08 improved with increasing canopy density for forests, whereas the opposite was observed for grass and crops. In general, site characteristics which increase dissimilarities between scalars (due to less mixing, large sink-source separation, coherent structures, ejections, etc.) appeared to enhance partitioning performance for SK10 and TH08.

For the forest site Loobos in The Netherlands, SK10 and TH08 obtained similar partitioning results and sufficient error metrics suggesting a low uncertainty. At this site with a relatively low leaf area index, high canopy, and low ratio between measurement and canopy height, conditions for both partitioning approaches seemed to be appropriate.

Appendix A

In Table A1 the number of half-hourly time steps during daylight per considered time period is shown for each study site. Also, the fraction of daylight time steps of high-quality (HQ) which were used in the application of SK10 and TH08 are shown, where for SK10 only a good or intermediate quality flag (after Mauder et al., 2013) and no precipitation were

required, and for TH08 additionally a negative $\rho_{q'c'}$. Furthermore, the fraction of these HQ-time steps, for which partitioning solutions were found, is shown for each method version. With TH08 by sampling in the first quadrant (Q1) a partitioning result could be obtained for almost every time step (minimum of 98.2%). With the hyperbolic threshold criterion and with GMM fewer solutions could be found, because quite often the number of sampled data points was less than 1% of the total number in one half-hour time period. SK10 sometimes could not find a partitioning solution, when the measured and estimated $\rho_{q'c'}$ were not equal and removing large-scale processes by Wavelet-transform could not help either to solve the system of equations. The most solutions were found for Forest_MMP and the least for Grass_RO, suggesting a dependence on vegetation height. For crop sites Maize_DI and SugarBeet_SE, the number of solutions with SK10 increased with development stage of the maize or sugar beet, respectively, while the ratio between measurement height and h_c decreased. At the same sites the number of solutions for TH08 with hyperbolic threshold and GMM decreased (the conditional sampling in Q1 was not affected). Generally, for the grasslands and the lower crop canopies more solutions were obtained with TH08 than SK10. An exception was the low intercrop in Selhausen (Intercrop_SE).

Supplement Link.

Competing interests. The authors declare that they have no conflict of interest.

Acknowledgements. This research was supported by the German Federal Ministry of Education and Research BMBF, project IDAS-GHG [grant number 01LN1313A]. The measurement infrastructure providing observational data was supported by the German Research Foundation DFG through the Transregional Collaborative Research Centre 32 (TR 32) and Terrestrial Environmental Observatories (TERENO). The authors thank all technicians, engineers, and laboratory assistances in TR32, TERENO, and elsewhere for providing measurements of the test sites. Finally, we thank the reviewer for their helpful and constructive comments that improved the quality of this manuscript.

References

Anderson, R.G., Zhang, X., and Skaggs, T.H.: Measurement and partitioning of evapotranspiration for application to vadose zone studies. Vadose Zone J. 16 (13), 1-9, doi:10.2136/vzj2017.08.0155, 2018.

Andreu, A., Kustas, W.P., Polo, M.J., Carrara, A., and González-Dugo, M.P.: Modeling surface energy fluxes over a dehesa (oak savanna) ecosystem using a thermal based two-source energy balance model (TSEB) I. Remote Sens. 10 (4), 567, 27 pp, doi:10.3390/rs10040567, 2018.

Babel, W., Lüers, J., Hübner, J., Rebmann, C., Wichura, B., Thomas, C.K., Serafimovich, A., and Foken, T.: Long-term carbon and water vapour fluxes. In: Foken, T. (Ed.): Energy and matter fluxes of a spruce forest ecosystem. Ecological Studies 229, Springer, 73-96, doi:10.1007/978-3-319-49389-3_4, 2017.

Baldocchi, D., Falge, E., Gu, L., Olson, R., Hollinger, D., Running, S., Anthoni, P., Bernhofer, C., Davis, K., Evans, R., Fuentes, J., Goldstein, A., Katul, G., Law, B., Lee, X., Malhi, Y., Meyers, T., Munger, W., Oechel, W., Paw U, K.T., Pilegaard, K., Schmid, H.P., Valentini, R., Verma, S., Vesala, T., Wilson, K., and Wofsy, S.: FLUXNET: A new tool to study the temporal and spatial variability of ecosystem-scale carbon dioxide, water vapor, and energy flux densities. Bull. Am. Meteorol. Soc. 82 (11), 2415-2434, doi:10.1175/1520-0477(2001)082<2415:FANTTS>2.3.CO;2, 2001.

Borchard, N., Schirrmann, M., von Hebel, C., Schmidt, M., Baatz, R., Firbank, L., Vereecken, H., and Herbst, M.: Spatio-temporal drivers of soil and ecosystem carbon fluxes at field scale in an upland grassland in Germany. Agric. Ecosyst. Environ. 211, 84-93, doi:10.1016/j.agee.2015.05.008, 2015.

Businger, J.A. and Oncley, S.P.: Flux measurement with conditional sampling. J. Atmos. Ocean. Technol. 7 (2), 349-352, doi:10.1175/1520-0426(1990)007<0349:FMWCS>2.0.CO;2, 1990.

Campbell, G.S. and Norman, J.M.: An introduction to environmental biophysics. New York: Springer, 286 pp, 1998.

Canty, M.J.: Image analysis, classification and change detection in remote sensing, with algorithms for ENVI/IDL. CRC Press, Boca Raton, FL, pp. 441, 2010.

Denmead, O.T., Dunin, F.X., Leuning, R., and Raupach, M.R.: Measuring and modelling soil evaporation in wheat crops. Phys. Chem. Earth 21 (3), 97-100, doi:10.1016/S0079-1946(97)85567-X, 1996.

Detto, M., and Katul, G.G.: Simplified expressions for adjusting higher-order turbulent statistics obtained from open path gas analyzers. Boundary-Layer Meteorol. 122 (1), 205-216, doi:10.1007/s10546-006-9105-1, 2007.

Dolman, A.J., Moors, E.J., and Elbers, J.A.: The carbon uptake of a mid latitude pine forest growing on sandy soil. Agric. For. Meteorol. 111 (3), 157-170, doi:10.1016/S0168-1923(02)00024-2, 2002.

Edburg, S.L., Stock, D., Lamb, B.K., and Patton, E.G.: The effect of the vertical source distribution on scalar statistics within and above a forest canopy. Boundary-Layer Meteorol. 142 (3), 365-382, doi:10.1007/s10546-011-9686-1, 2012.

Eder, F., Schmidt, M., Damian, T., Träumer, K., and Mauder, M.: Mesoscale eddies affect near-surface turbulent exchange: evidence from Lidar and tower measurements. J. Appl. Meteorol. Clim. 54 (1), 189-206, https://doi.org/10.1175/JAMC-D-14-0140.1, 2015.

Elbers, J.A., Jacobs, C.M.J., Kruijt, B., Jans, W.W.P., and Moors, E.J.: Assessing the uncertainty of estimated annual totals of net ecosystem productivity: A practical approach applied to a mid latitude temperate pine forest. Agric. For. Meteorol. 151 (12), 1823-1830, doi:10.1016/j.agrformet.2011.07.020, 2011.

Falge, E., Baldocchi, D., Tenhunen, J., Aubinet, M., Bakwin, P., Berbigier, P., Bernhofer, C., Burba, G., Clement, R., Davis, K.J., Elbers, J.A., Goldstein, A.H., Grelle, A., Granier, A., Guðmundsson, J., Hollinger, D., Kowalski, A.S., Katul, G., Law, B.E., Malhi, Y., Meyers, T., Monson, R.K., Munger, J.W., Oechel, W., Paw U, K.T., Pilegaard, K., Rannik, Ü., Rebmann, C., Suyker, A., Valentini, R., Wilson, K., and Wofsy, S.: Seasonality of ecosystem respiration and gross primary production as derived from FLUXNET measurements. Agric. For. Meteorol. 113 (1-4), 53-74, doi:10.1016/S0168-1923(02)00102-8, 2002.

Foken, T., Gerstberger, P., Köck, K., Siebicke, L., Serafimovich, A., and Lüers, J.: Description of the Waldstein measuring site. In: Foken, T. (Ed.), 2017. Energy and matter fluxes of a spruce forest ecosystem. Ecological Studies 229, Springer, 19-38, doi:10.1007/978-3-319-49389-3_2, 2017.

Gebler, S., Hendricks Franssen, H.-J., Pütz, T., Post, H., Schmidt, M., and Vereecken, H.: Actual evapotranspiration and precipitation measured by lysimeters: a comparison with eddy covariance and tipping bucket. Hydrol. Earth Syst. Sci. 19 (5), 2145-2161, doi:10.5194/hess-19-2145-2015, 2015.

Good, S.P., Soderberg, K., Guan, K., King, E.G., Scanlon, T.M., and Caylor, K.K.: δ^2H isotopic flux partitioning of evapotranspiration over a grass field following a water pulse and subsequent dry down. Water Resour. Res. 50 (2), 1410-1432, doi:10.1002/2013WR014333, 2014.

Good, S.P., Noone, D., Bowen, G.: Hydrologic connectivity constrains partitioning of global terrestrial water fluxes. Sciences 349 (6244), 175-177, doi:10.1126/science.aaa5931, 2015.

Graf, A., Bogena, H.R., Drüe, C., Hardelauf, H., Pütz, T., Heinemann, G., and Vereecken, H.: Spatiotemporal relations between water budget components and soil water content in a forested tributary catchment. Water Resour. Res. 50 (6), 4837-4857, doi:10.1002/2013WR014516, 2014.

Huang, J., Katul, G., and Albertson, J.: The role of coherent turbulent structures in explaining scalar dissimilarity within the canopy sublayer. Environ. Fluid Mech. 13 (6), 571-599, doi:10.1007/s10652-013-9280-9, 2013.

Jans, W.W.P., Jacobs, C.M.J., Kruijt, B., Elbers, J.A., Barendse, S., and Moors, E.J.: Carbon exchange of a maize (Zea mays L.) crop: Influence of phenology. Agric. Ecosyst. Environ. 139 (3), 316-324, doi:10.1016/j.agee.2010.06.008, 2010.

Jin, H., Eklundh, L.: A physically based vegetation index for improved monitoring of plant phenology. Remote Sens. Environ. 152, 512-525, doi:10.1016/j.rse.2014.07.010, 2014.

Klosterhalfen, A., Moene, A.F., Schmidt, M., Scanlon, T.M., Vereecken, H., and Graf, A.: Sensitivity Analysis of a source partitioning method for H_2O and CO_2 fluxes based on high frequency eddy covariance data: findings from field data and large eddy simulations. Agric. For. Meteorol. 265, 152-170, doi:10.1016/j.agrformet.2018.11.003, 2019.

Li, X., Gentine, P., Lin, C., Zhou, S., Sun, Z., Zheng, Y., Liu, J., Zheng, C.: A simple and objective method to partition evapotranspiration into transpiration and evaporation at eddy-covariance sites. Agric. For. Meteorol. 265, 171-182, doi:10.1016/j.agrformet.2018.11.017, 2019.

Lindauer, M., Schmid, H.P., Grote, R., Mauder, M., Steinbrecher, R., and Wolpert, B.: Net ecosystem exchange over a non-cleared wind-throw-disturbed upland spruce forest - Measurements and simulations. Agric. For. Meteorol. 197, 219-234, doi:10.1016/j.agrformet.2014.07.005, 2014.

Linderson, M.-L., Mikkelsen, T.N., Ibrom, A., Lindroth, A., Ro-Poulsen, H., Pilegaard, K.: Up-scaling of water use efficiency from leaf to canopy as based on leaf gas exchange relationships and the modeled in-canopy light distribution. Agric. For. Meteorol. 152, 201-211, doi:10.1016/j.agrformet.2011.09.019, 2012.

Lloyd, J., and Taylor, A.: On the temperature dependence of soil respiration. Funct. Ecol. 8 (3), 315-323, doi:10.2307/2389824, 1994.

Matiu, M., Bothmann, L., Steinbrecher, R., and Menzel, A.: Monitoring succession after a non-cleared windthrow in a Norway spruce mountain forest using webcam, satellite vegetation indices and turbulent CO2 exchange. Agric. For. Meteorol. 244-245, 72-81, doi:10.1016/j.agrformet.2017.05.020, 2017.

Mauder, M., Cuntz, M., Drüe, C., Graf, A., Rebmann, C., Schmid, H.P., Schmidt, M., and Steinbrecher, R.: A strategy for quality and uncertainty assessment of long-term eddy-covariance measurements. Agric. For. Meteorol. 169, 122-135, doi:10.1016/j.agrformet.2012.09.006, 2013.

Ney, P., and Graf, A.: High-resolution vertical profiles measurements for carbon dioxide and water vapour concentrations within and above crop canopies. Boundary-Layer Meteorol. 166 (3), 449-473, doi:10.1007/s10546-017-0316-4, 2018.

Ney, P., Graf, A., Bogena, H., Diekkrüger, B., Drüe, C., Esser, O., Heinemann, G., Klosterhalfen, A., Pick, K., Pütz, T., Schmidt, M., Valler, V., and Vereecken, H.: CO_2 fluxes before and after partially deforestation of a Central European spruce forest. Agric. For. Meteorol., in review.

Palatella, L., Rana, G., and Vitale, D.: Towards a flux-partitioning procedure based on the direct use of high-frequency eddy-covariance data. Boundary-Layer Meteorol. 153 (2), 327-337, doi:10.1007/s10546-014-9947-x, 2014.

Reichstein, M., Falge, E., Baldocchi, D., Papale, D., Aubinet, M., Berbigier, P., Bernhofer, C., Buchmann, N., Gilmanov, T., Granier, A., Grünwald, T., Havránková, K., Ilvesniemi, H., Janous, D., Knohl, A., Laurila, T., Lohila, A., Loustau, D., Matteucci, G., Meyers, T., Miglietta, F., Ourcival, J.-M., Pumpanen, J., Rambal, S., Rotenberg, E., Sanz, M., Tenhunen, J., Seufert, G., Vaccari, F., Vesala, T., Yakir, D., and Valentini, R.: On the separation of net ecosystem exchange into assimilation and ecosystem respiration: review and improved algorithm. Global Change Biol. 11 (9), 1424-1439, doi:10.1111/j.1365-2486.2005.001002.x, 2005.

Reichstein, M., Stoy, P.C., Desai, A.R., Lasslop, G., and Richardson, A.D.: Partitioning of net fluxes. In: Aubinet, M., Vesala, T., and Papale, D. (Eds.): Eddy covariance. A practical guide to measurement and data analysis. Dordrecht, Heidelberg, London, New York: Springer, pp. 263-289, 2012.

Scanlon, T.M., and Albertson, J.D.: Turbulent transport of carbon dioxide and water vapor within a vegetation canopy during unstable conditions: Identification of episodes using wavelet analysis. J. Geophys. Res. 106 (D7), 7251-7262, doi:10.1029/2000JD900662, 2001.

Scanlon, T.M., and Kustas, W.P.: Partitioning carbon dioxide and water vapor fluxes using correlation analysis. Agric. For. Meteorol. 150 (1), 89-99, doi:10.1016/j.agrformet.2009.09.005, 2010.

Scanlon, T.M., and Kustas, W.P.: Partitioning evapotranspiration using an eddy covariance-based technique: Improved assessment of soil moisture and land-atmosphere exchange dynamics. Vadose Zone J. 11 (3), 12 pp, doi:10.2136/vzj2012.0025, 2012.

Scanlon, T.M., and Sahu, P.: On the correlation structure of water vapor and carbon dioxide in the atmospheric surface layer: A basis for flux partitioning. Water Resour. Res. 44 (10), W10418, 15 pp, doi:10.1029/2008WR006932, 2008.

Schlesinger, W.H., Jasechko, S.: Transpiration in the global water cycle. Agric. For. Meteorol. 189-190, 115-117, doi:10.1016/j.agrformet.2014.01.011, 2014.

Skaggs, T.H., Anderson, R.G., Alfieri, J.G., Scanlon, T.M., Kustas, W.P.: Fluxpart: Open source software for partitioning carbon dioxide and water vapor fluxes. Agric. For. Meteorol. 253-254, 218-224, doi:10.1016/j.agrformet.2018.02.019, 2018.

Špunda, V., Kalina, J., Urban, O., Luis, V.C., Sibisse, I., Puértolas, J., Šprtová, M., and Marek, M.V.: Diurnal dynamics of photosynthetic parameters of Norway spruce trees cultivated under ambient and elevated CO_2: the reasons of midday depression in CO_2 assimilation. Plant Sci. 168 (5), 1371-1381, doi:10.1016/j.plantsci.2005.02.002, 2005.

Sulman, B.N., Roman, D.T., Scanlon, T.M., Wang, L., and Novick, K.A.: Comparing methods for partitioning a decade of carbon dioxide and water vapor fluxes in a temperate forest. Agric. For. Meteorol. 226-227, 229-245, doi:10.1016/j.agrformet.2016.06.002, 2016.

Thomas, C., Martin, J.G., Goeckede, M., Siqueira, M.B., Foken, T., Law, B.E., Loescher, H.W., and Katul, G.: Estimating daytime subcanopy respiration from conditional sampling methods applied to multi-scalar high frequency turbulence time series. Agric. For. Meteorol. 148 (8-9), 1210-1229, doi:10.1016/j.agrformet.2008.03.002, 2008.

Thomas, C.K., Law, B.E., Irvine, J., Martin, J.G., Pettijohn, J.C., and Davis, K.J.: Seasonal hydrology explains interannual and seasonal variation in carbon and water exchange in a semiarid mature ponderosa pine forest in central Oregon. J. Geophys. Res. 114, G04006, 22 pp, doi:10.1029/2009JG001010, 2009.

Vickers, D., Thomas, C.K., Pettijohn, C., Martin, J.G., and Law, B.E.: Five years of carbon fluxes and inherent water-use efficiency at two semi-arid pine forests with different disturbance histories. Tellus B Chem. Phys. Meteorol. 64, 17159, 14 pp, doi:10.3402/tellusb.v64i0.17159, 2012.

Wang, W., Smith, J.A., Ramamurthy, P., Baeck, M.L., Bou-Zeid, E., and Scanlon, T.M.: On the correlation of water vapor and CO_2: application to flux partitioning of evapotranspiration. Wat. Resour. Res. 52 (12), 9452-9469, doi:10.1002/2015WR018161, 2016.

Webster, R.: Regression and functional relations. Eur. J. Soil. Sci. 48 (3), 557-566, doi:10.1111/j.1365-2389.1997.tb00222.x, 1997.

Wiekenkamp, I., Huisman, J.A., Bogena, H.R., Graf, A., Lin, H.S., Drüe, C., and Vereecken, H.: Changes in measured spatiotemporal patterns of hydrological response after partial deforestation in a headwater catchment. J. Hydrol. 542, 648-661, doi:10.1016/j.jhydrol.2016.09.037, 2016.

Williams, M., Rastetter, E.B., Fernandes, D.N. Goulden, M.L., Wofsy, S.C., Shaver, G.R., Melillo, J.M., Munger, J.W., Fan, S.-M., and Nadelhoffer, K.J.: Modelling the soil-plant-atmosphere continuum in a Quercus-Acer stand at Harvard Forest: the regulation of stomatal conductance by light, nitrogen and soil/plant hydraulic properties. Plant Cell Environ. 19 (8), 911-927, doi:10.1111/j.1365-3040.1996.tb00456.x, 1996.

Williams, C.A., Scanlon, T.M., and Albertson, J.D.: Influence of surface heterogeneity on scalar dissimilarity in the roughness sublayer. Boundary-Layer Meteorol. 122 (1), 149-165, doi:10.1007/s10546-006-9097-x, 2007.

Wollschläger, U., Attinger, S., Borchardt, D., Brauns, M., Cuntz, M., Dietrich, P., Fleckenstein, J.H., Friese, K., Friesen, J., Harpke, A., Hildebrandt, A., Jäckel, G., Kamjunke, N., Knöller, K., Kögler, S., Kolditz, O., Krieg, R., Kumar, R., Lausch, A., Liess, M., Marx, A., Merz, R., Mueller, C., Musolff, A., Norf, H., Oswald, S.E., Rebmann, C., Reinstorf, F., Rode, M.,

Rink, K., Rinke, K., Samaniego, L., Vieweg, M., Vogel, H.-J., Weitere, M., Werban, U., Zink, M., and Zacharias, S.: The Bode hydrological observatory: a platform for integrated, interdisciplinary hydro-ecological research within the TERENO Harz/Central German Lowland Observatory. Environ. Earth Sci. 76 (1), 29, 25 pp, doi:10.1007/s12665-016-6327-5, 2017.

Xue, Q., Weiss, A., Arkebauer, T.J., and Baenziger, P.S.: Influence of soil water status and atmospheric vapor pressure deficit on leaf gas exchange in field-grown winter wheat. Environ. Exp. Bot. 51 (2), 167-179, doi:10.1016/j.envexpbot.2003.09.003, 2004.

Zeeman, M.J., Eugster, W., and Thomas, C.K.: Concurrency of coherent structures and conditionally sampled daytime sub-canopy respiration. Boundary-Layer Meteorol. 146, 1-15, doi:10.1007/s10546-012-9745-2, 2013.

Zeeman, M.J., Mauder, M., Steinbrecher, R., Heidbach, K. Eckart, E., and Schmid, H.P.: Reduced snow cover affects productivity of upland temperate grasslands. Agric. For. Meteorol. 232, 514-526, doi:10.1016/j.agrformet.2016.09.002, 2017.
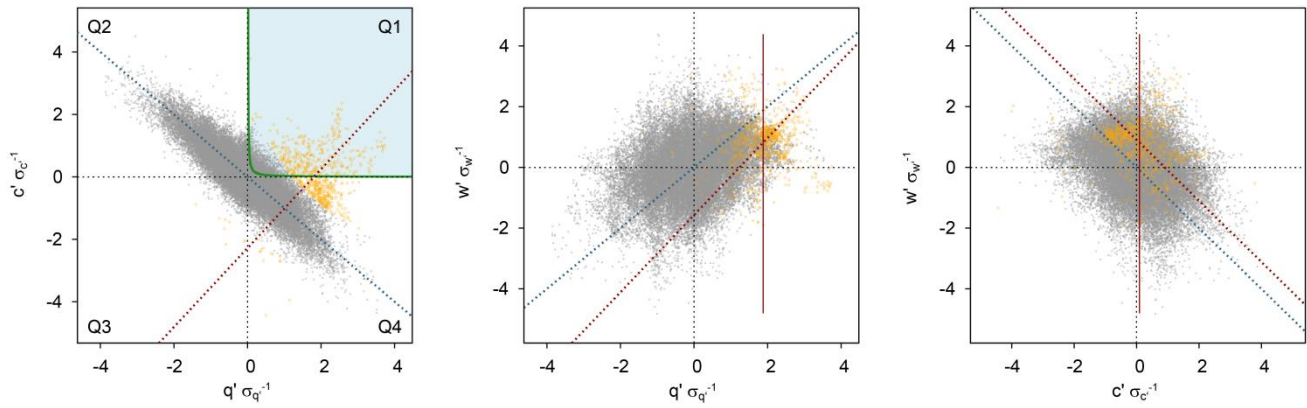
Figure 1: Exemplary scatterplots of *w'*, *q'*, and *c'* from the Wüstebach study site (forest), 18 May 2015, 12:00-12:30 p.m. including results of the cluster analysis by Gaussian Mixture Model (orange data points) for the conditional sampling. Also shown are the hyperbolic threshold (H = 0.25, green line) after Thomas et al. (2008), the averages of *q* and *c* only considering data points of the respiration/evaporation 'cloud' (red lines), and reduced major axis regression lines after Webster (1997) for all data points (blue dashed lines) and only 'cloud' data points (red dashed lines).

In this example, calculating the covariance for *w* and *c* considering the CO_2 average of the 'cloud' yielded a negative soil flux (negative correlation). Thus, only 'cloud' data points within quadrant 1 in the original *q'*-*c'* plane were considered for flux calculation using averages of all data points.
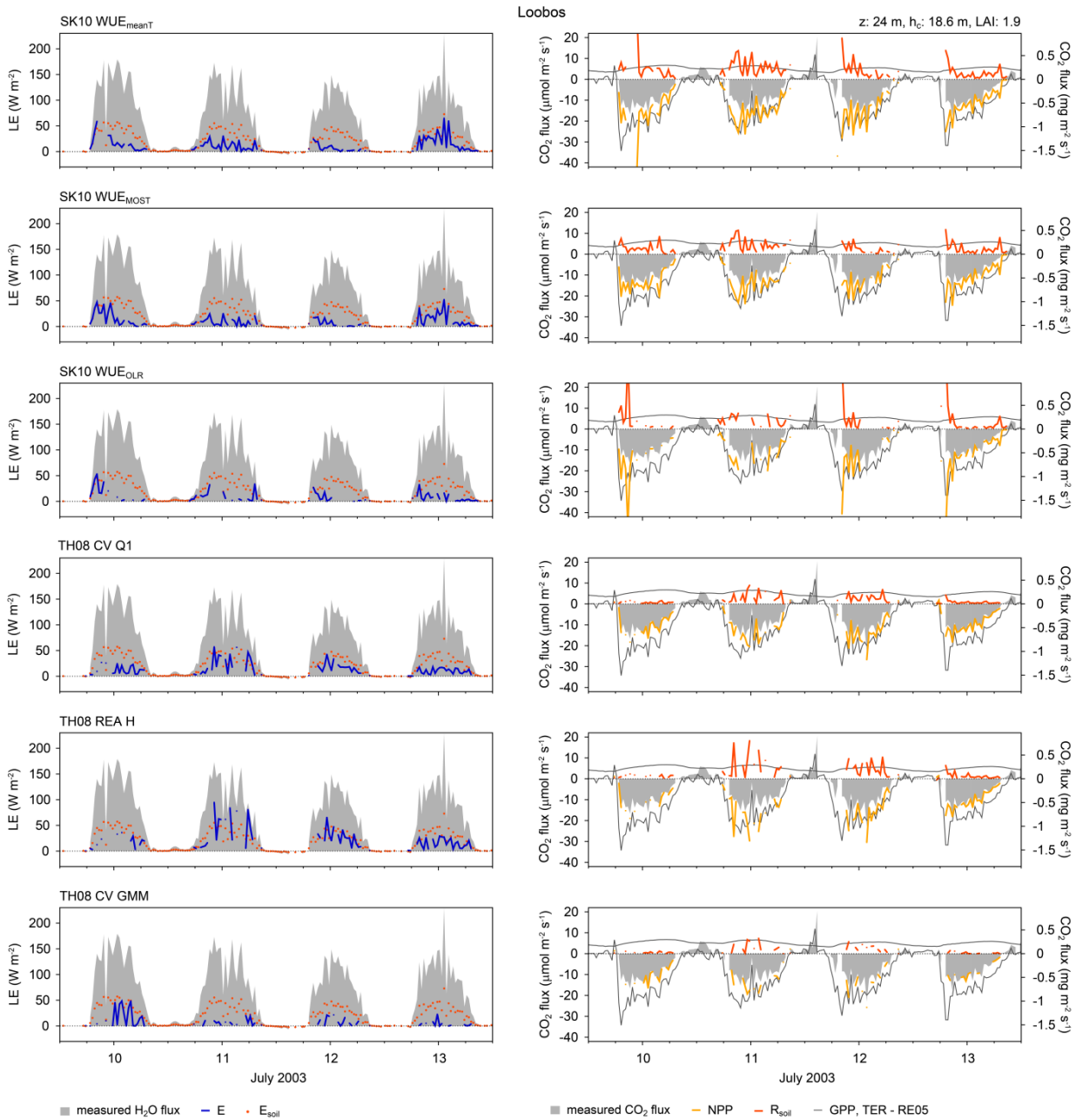
Figure 2: Source partitioning results of H$_2$O (left) and CO$_2$ (right) fluxes in half-hourly time steps for the Loobos study site (forest) in The Netherlands. The figure shows four days out of the considered time period and selected method versions (see text for description). Results of all days and for every method version are shown in the supplementary material. Grey areas show the measured water and CO$_2$ fluxes. Soil evaporation estimates derived based on Beer's law and CO$_2$ flux estimates by Reichstein et al. (2005; RE05) are also included (LE: latent heat flux; E: evaporation; E$_{soil}$: estimated soil evaporation; GPP: gross primary production; NPP: net primary production; TER: total ecosystem respiration; R$_{soil}$: soil respiration; z: measurement height; h$_c$: canopy height; LAI: leaf area index).
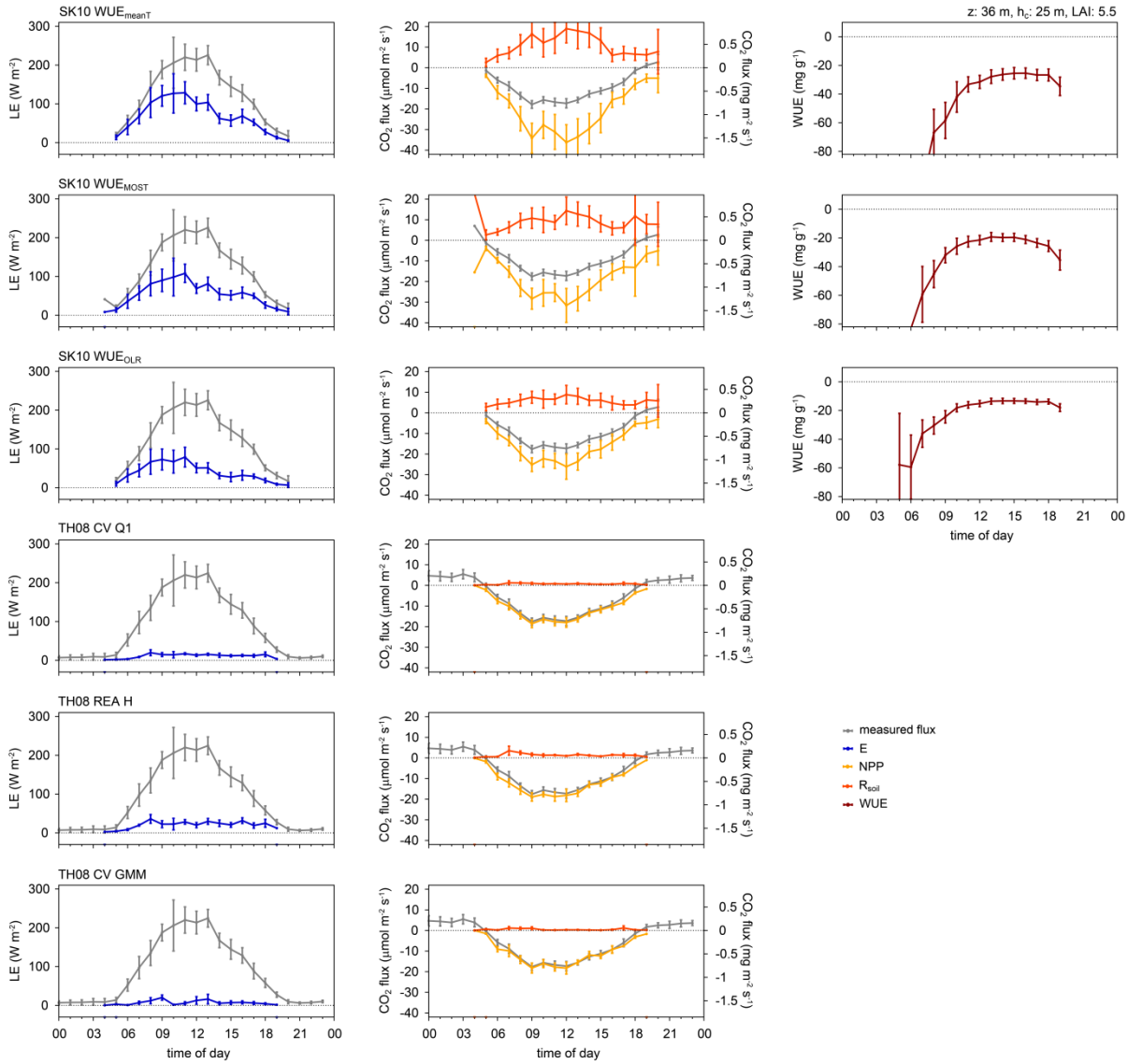
Figure 3: Diurnal dynamics of source partitioning results of H₂O (left) and CO₂ (middle) fluxes and water use efficiency (WUE, right) for the Waldstein study site (forest) in Germany for 4-10 July, 2016 and for selected method versions (see text for description; LE: latent heat flux; E: evaporation; NPP: net primary production; R_{soil}: soil respiration; z: measurement height; h_c: canopy height; LAI: leaf area index). Error bars indicate the 95% confidence intervals of the mean values.
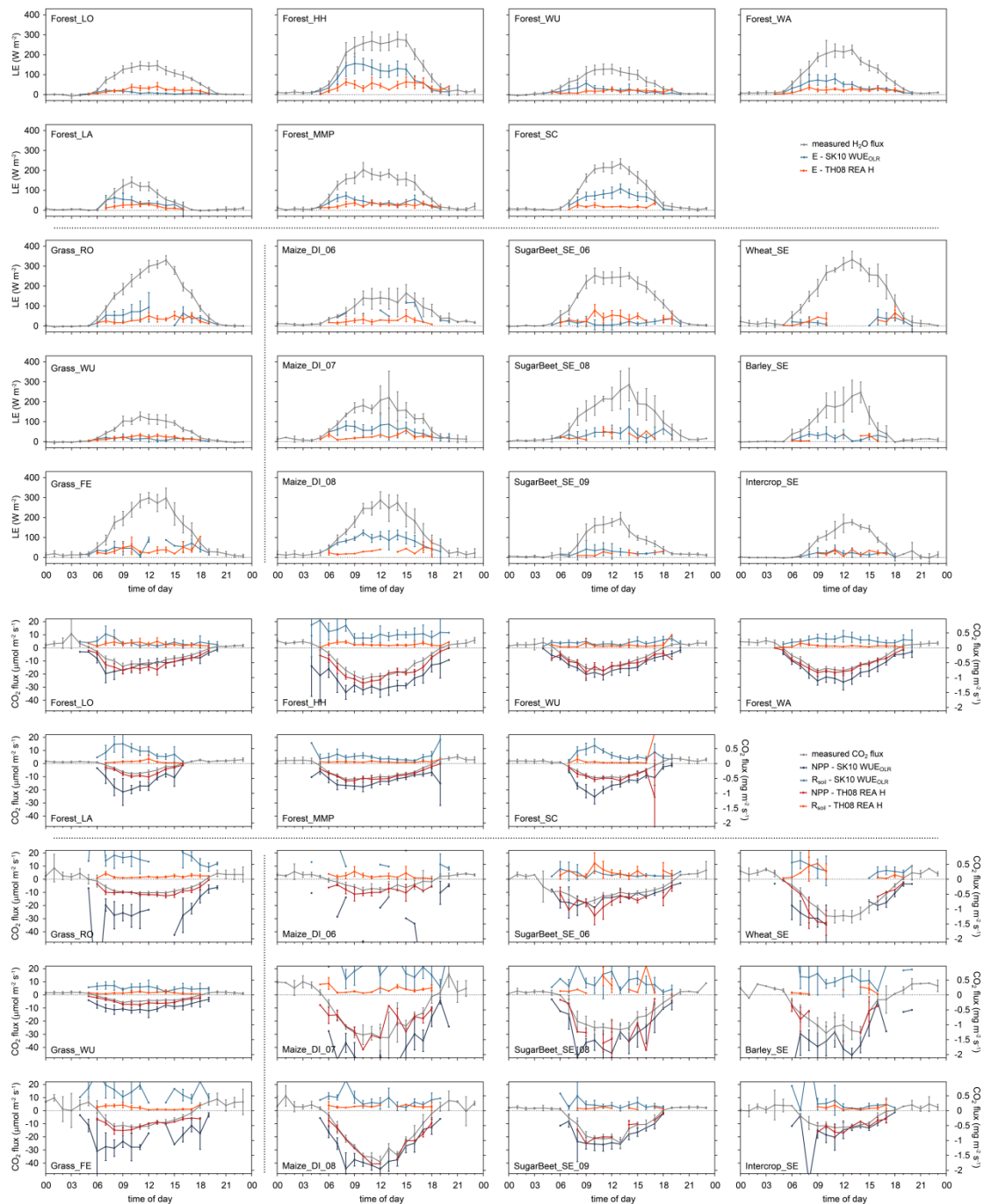
Figure 4: Diurnal dynamics of source partitioning results of H_2O (upper panels) and CO_2 (lower panels) fluxes for all study sites and for the approach after Scanlon and Kustas (2010; SK10) with WUE_{OLR} and after Thomas et al. (2008; TH08) with REA H (see text for description; LE: latent heat flux; E: evaporation; NPP: net primary production; R_{soil}: soil respiration). Error bars indicate the 95% confidence intervals of the mean values.
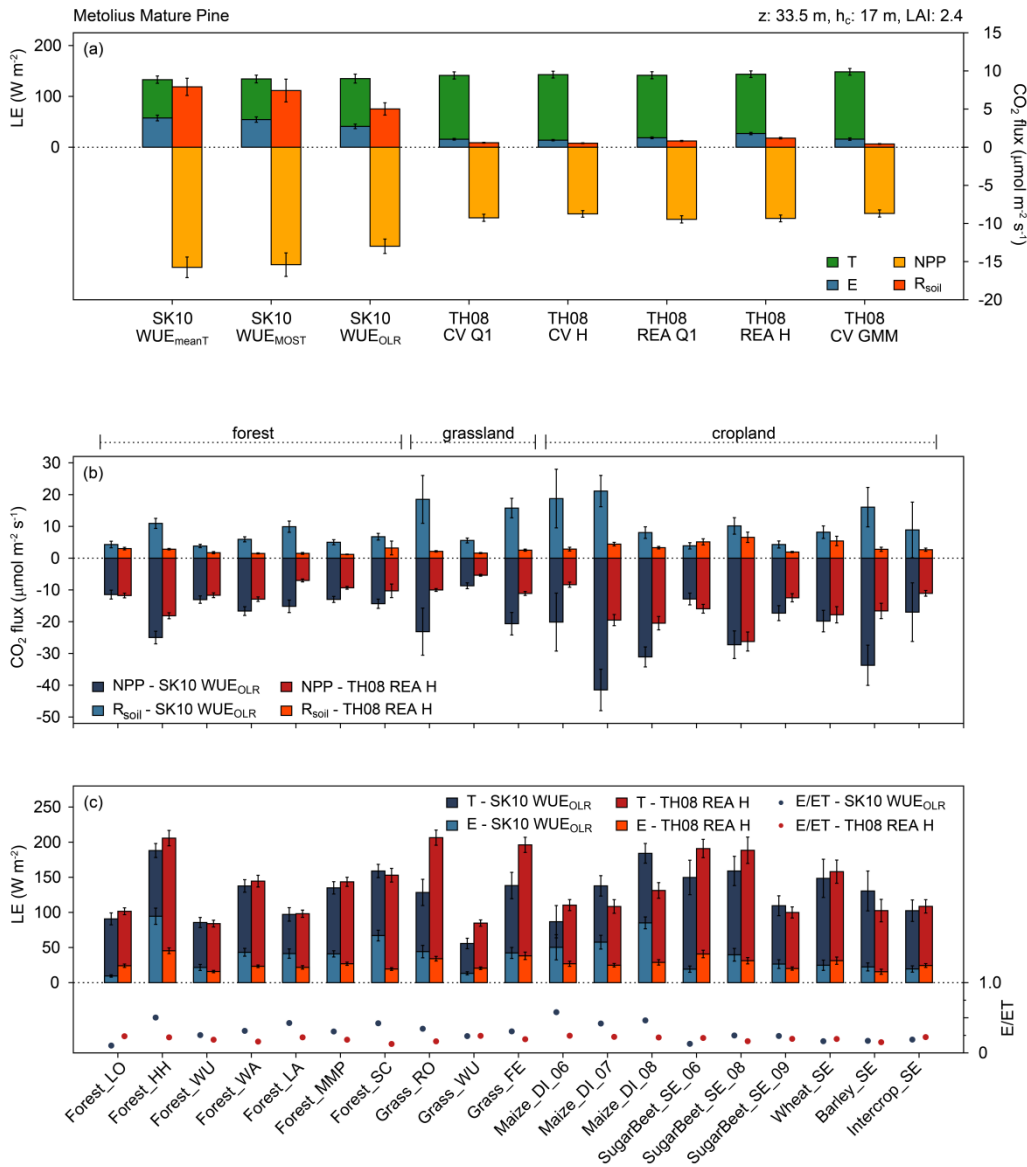
Figure 5: Averages of source partitioning results (a) of H₂O and CO₂ fluxes, for the Metolius Mature Pine study site (forest) in US and for all method versions, (b) of CO₂ fluxes, for all study sites and for the approaches after Scanlon and Kustas (2010; SK10) with WUE_OLR and after Thomas et al. (2008; TH08) with REA H, and (c) of H₂O fluxes and the partitioning fraction E/ET, for all study sites and for the approaches SK10 WUE_OLR and TH08 REA H (see text for description; LE: latent heat flux; E: evaporation; NPP: net primary production; R_soil: soil respiration; z: measurement height; h_c: canopy height; LAI: leaf area index). Error bars indicate the 95% confidence intervals of the mean values. For each study site, net fluxes (evapotranspiration and net ecosystem exchange) differ between method versions, because each method version found a different number of partitioning solutions, thus, the averages were taken from different subsets of the original data.
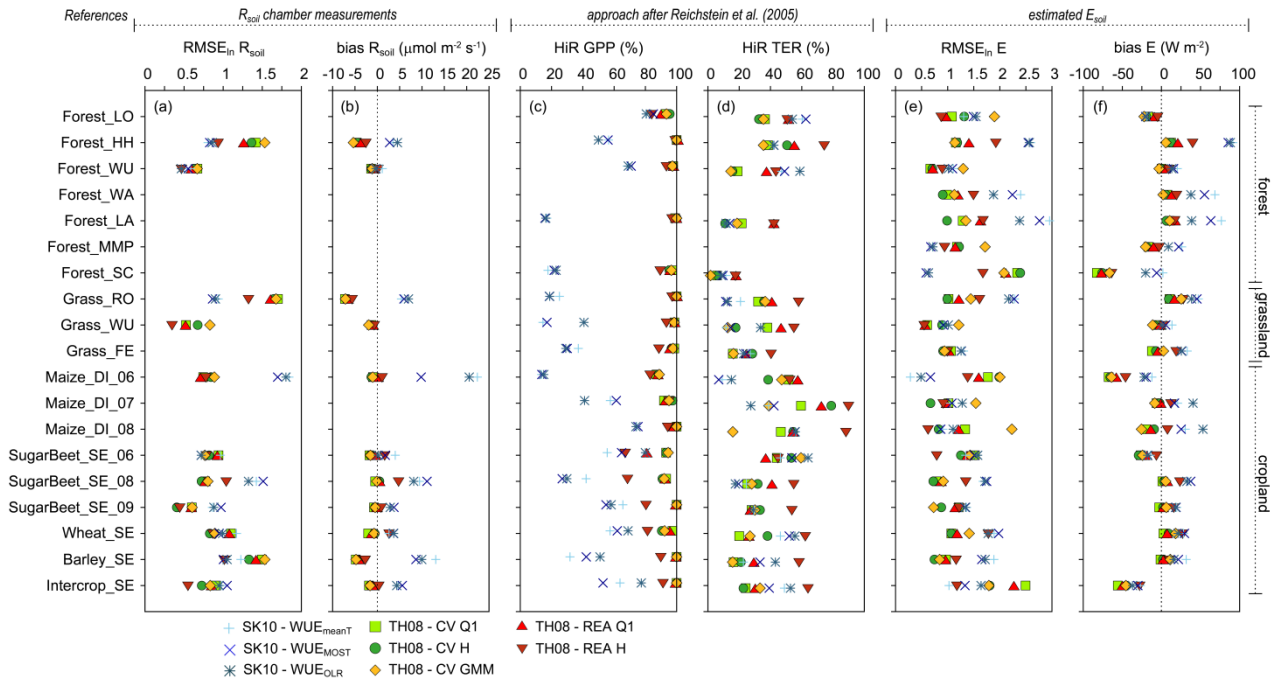
Figure 6: Error metrics of source partitioning results for each study site and method version (see text for description). (a)-(b) Root mean square error in log-transformed data (RMSE$_{ln}$) and bias considering soil respiration (R$_{soil}$) chamber measurements, (c)-(d) percent fraction of time steps with partitioning results in range (HiR) of estimated gross primary production (GPP) and total ecosystem respiration (TER) by the approach after Reichstein et al. (2005), (e)-(f) RMSE$_{ln}$ and bias considering soil evaporation (E$_{soil}$) estimated based on Beer's law.
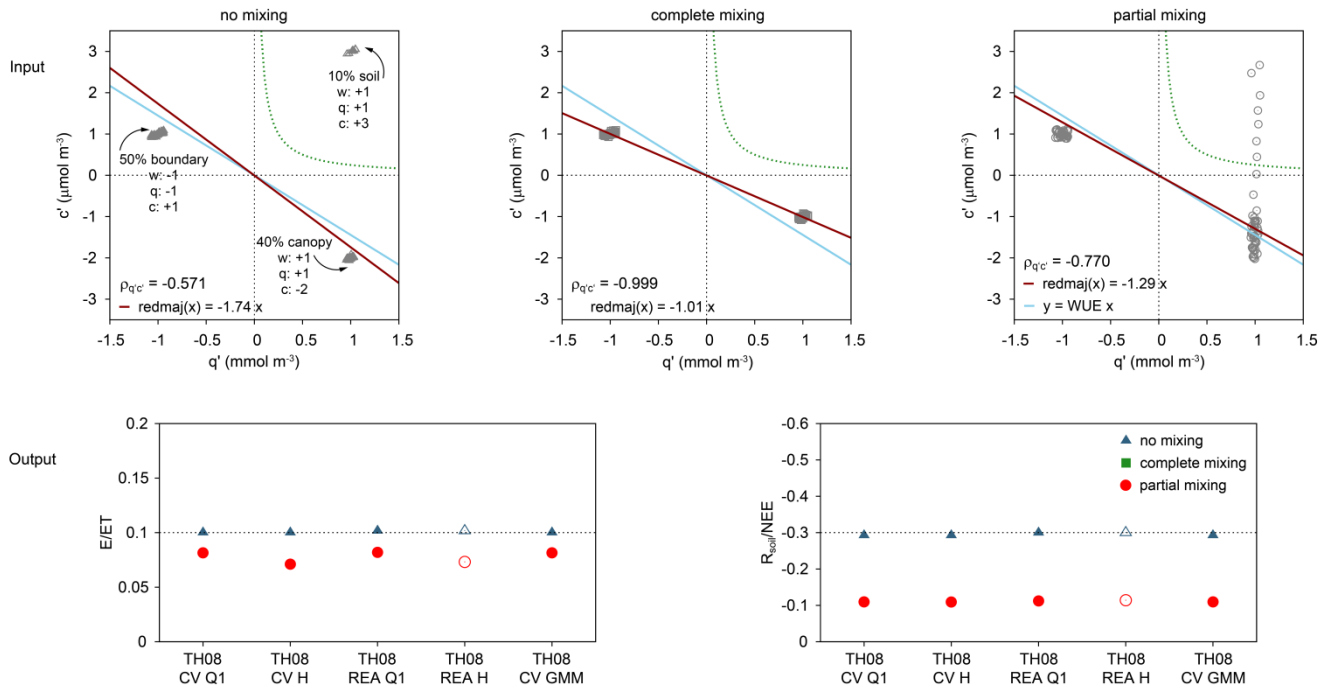
Figure 7: Top: Setup of conceptual model for synthetic fluctuations (*q'* and *c'*) originating from soil, canopy, or boundary layer with differing degrees of mixing (no, complete, or partial mixing between soil and canopy sink/source) including water use efficiency (WUE = -1.444 μmol mmol^{-1} = -3.53 mg g^{-1}; blue line), reduced major axis regression (red line) after Webster (1997), hyperbolic threshold criterion after Thomas et al. (2008; TH08) (H = 0.25; green dashed line) and correlation coefficient between *q'* and *c'* ($\rho_{q'c'}$). **Bottom:** True known partitioning ratios (dashed line) and source partitioning results of all TH08 method versions (see text for description) for each degree of mixing.

Table 1: Study sites and their characteristics (organized by first canopy type and second latitude; FR: forest; GL: grassland; CL: cropland).

abbreviation	site	Latitude Longitude	elevation (m a.s.l.)	canopy type	period	LAI ($m^2\ m^{-2}$)	canopy height (m)	EC meas height (m)	mean annual Temp (°C)	mean annual P sum (mm a^{-1})	prevailing wind direction	references
Forest_LO	**Loobos** Netherlands	52.1666 5.7436	25	**FR** (pine)	08.-14. July 2003	1.9	18.6	24.0	10.0	966	W-SW	Dolman et al., 2002 Elbers et al., 2011
Forest_HH	**Hohes Holz** Germany	52.0853 11.2222	210	**FR** (deciduous broadleaf)	03.-09. July 2016	6.0	33.0	49.0	9.8	516	SW	Wollschläger et al., 2017
Forest_WU	**Wüstebach (forest)** Germany	50.5049 6.3310	610	**FR** (spruce)	18.-24. May 2015	3.9	25.0	38.0	7.5	1220	SSW	Ney et al., in review Graf et al., 2014
Forest_WA	**Waldstein** Germany	50.1419 11.8669	775	**FR** (spruce)	04.-10. July 2016	5.5	25.0	36.0	5.8	885	SSW	Babel et al., 2017 Foken et al., 2017
Forest_LA	**Lackenberg** Germany	49.0996 13.3047	1308	**FR** (spruce/grass)	24.-30. September 2017	6.0[*]	3.0	9.0	3.7	1480	SSW	Lindauer et al., 2014 Matiu et al., 2017
Forest_MMP	**Metolius Mature Pine** Oregon, USA	44.4523 -121.5574	1253	**FR** (pine)	06.-12. June 2014	2.4	17.0	33.5	6.3	523	SSW	Thomas et al., 2009 Vickers et al., 2012
Forest_SC	**Sta. Clotilde** Spain	38.2101 -4.2875	736	**FR** (oak savanna)	01.-07. April 2017	1.0	8.5	18.0	15.3	720	SW	Andreu et al., 2018
Grass_RO	**Rollesbroich** Germany	50.6219 6.3041	515	**GL**	15.-21. July 2013	5.9	0.19	2.6	7.7	1033	SSW	Borchard et al., 2015 Gebler et al., 2015
Grass_WU	**Wüstebach (clear cut)** Germany	50.5030 6.3359	610	**GL** (deforested area)	18.-24. May 2015	< 2.5	0.25	2.5	7.5	1220	SSW	Ney et al., in review Wiekenkamp et al., 2016
Grass_FE	**Fendt** Germany	47.8329 11.0607	595	**GL**	11.-17. July 2015	3.5	0.25	3.5	8.4	1081	SW	Zeeman et al., 2017
Maize_DI_06 **Maize_DI_07** **Maize_DI_08**	**Dijkgraaf** Netherlands	51.9921 5.6459	9	**CL** (maize)	14.-16. June 2007 14.-16. July 2007 04.-06. August 2007	0.35 3.5 3.0	0.35 1.70 2.80	4.0	10.5	803	S-SW	Jans et al., 2010
Wheat_SE **Barley_SE** **Intercrop_SE** **SugarBeet_SE_06** **SugarBeet_SE_08** **SugarBeet_SE_09**	**Selhausen** Germany	50.8658 6.4474	103	**CL** (winter wheat) (barley) (intercrop) (sugar beet)	03.-05. June 2015 27.-29. May 2016 23.-25. September 2016 20.-22. June 2017 02.-04. August 2017 04.-06. September 2017	6.1 5.1 1.0 2.3 5.2 4.3	0.79 0.95 0.22 0.37 0.46 0.50	2.4	9.9	698	WSW	Eder et al., 2015 Ney and Graf, 2018

LAI: leaf area index; EC: eddy covariance; meas: measurement; T: temperature; P: precipitation
[*] LAI estimated based on remotely sensed plant phenology index (PPI; Matiu et al., 2017) and approach after Jin and Eklundh (2014)

Table 2: Correlation coefficients between partitioning performance of each method version regarding HiR GPP (see text for description) and study site characteristics (h_c: canopy height; LAI: leaf area index; z: measurement height) considering different sets of sites: all, only forest, or only crop- and grassland sites. Bold lettering indicates highest positive and highest negative correlation. Underlined lettering indicates highest magnitude of correlation and italic lettering lowest magnitude of correlation. Also, the statistical significance of the correlations is indicated with one asterisk for $p \leq 0.1$ and two asterisks for $p \leq 0.05$.

variable	SK10 WUE$_{meanT}$	SK10 WUE$_{MOST}$	SK10 WUE$_{OLR}$	TH08 CV Q1	TH08 CV H	TH08 REA Q1	TH08 REA H	TH08 CV GMM
all								
h_c	**0.52** **	**0.56** **	**0.44** *	0.21	0.27	0.28	0.45 *	0.23
LAI	*0.04*	*0.01*	*-0.08*	**0.44** *	0.25	**0.45** *	0.17	**0.30**
z	0.48 **	0.52 **	0.40 *	0.23	**0.27**	0.31	**0.48** **	0.25
z h_c^{-1}	**-0.51** **	**-0.60** **	**-0.45** *	*-0.11*	-0.15	-0.13	-0.15	-0.10
LAI h_c^{-1}	-0.38	-0.47 **	-0.41 *	0.18	*0.03*	*0.09*	*-0.13*	*0.09*
forests								
h_c	**0.64**	**0.63**	**0.56**	0.20	*0.21*	*0.21*	0.27	*0.11*
LAI	*-0.03*	*-0.07*	*-0.10*	**0.61**	**0.77** **	**0.68** *	**0.69** *	**0.69** *
z	0.62	0.60	0.55	0.37	0.31	0.36	0.41	0.27
z h_c^{-1}	**-0.74** *	**-0.75** *	**-0.68** *	0.27	0.25	0.28	*0.20*	0.37
LAI h_c^{-1}	-0.59	-0.61	-0.59	*0.19*	0.38	0.26	0.22	0.36
croplands, grasslands								
h_c	**0.54** *	**0.64** **	**0.33**	0.07	**0.23**	0.12	0.31	0.16
LAI	0.07	*0.05*	-0.10	**0.40**	0.10	**0.37**	*-0.03*	0.15
z	*0.02*	0.07	-0.29	**-0.44**	-0.11	-0.17	**0.37**	-0.23
z h_c^{-1}	**-0.58** **	**-0.71** **	**-0.51** *	*-0.01*	-0.01	*0.03*	0.17	*0.03*
LAI h_c^{-1}	-0.37	-0.49	-0.46	0.37	0.21	0.32	0.16	**0.28**

Table 3: Correlation coefficients between partitioning performance of each method version regarding HiR TER (see text for description) and study site characteristics (h_c: canopy height; LAI: leaf area index; z: measurement height) considering different sets of sites: all, only forest, or only crop- and grassland sites. Bold lettering indicates highest positive and highest negative correlation. Underlined lettering indicates highest magnitude of correlation and italic lettering lowest magnitude of correlation. Also, the statistical significance of the correlations is indicated with one asterisk for $p \leq 0.1$ and two asterisks for $p \leq 0.05$.

variable	SK10 WUE$_{meanT}$	SK10 WUE$_{MOST}$	SK10 WUE$_{OLR}$	TH08 CV Q1	TH08 CV H	TH08 REA Q1	TH08 REA H	TH08 CV GMM
all								
h_c	**0.52****	**0.52****	**0.47****	-0.12	-0.18	**0.17**	*0.01*	-0.23
LAI	*0.01*	0.06	-0.03	**-0.20**	0.04	*-0.01*	**0.24**	*-0.12*
z	0.48**	0.47**	0.44*	-0.17	**-0.24**	0.12	-0.06	**-0.27**
z h_c^{-1}	**-0.47****	**-0.57****	**-0.42***	**0.08**	*-0.01*	-0.14	**-0.15**	**0.30**
LAI h_c^{-1}	-0.37	-0.44*	-0.41*	*-0.06*	**0.06**	**-0.21**	-0.04	0.18
forests								
h_c	**0.63**	**0.63**	0.63	**0.59**	**0.68***	0.56	**0.76****	**0.43**
LAI	*-0.02*	*0.02*	*0.05*	0.43	0.31	**0.61**	0.65	0.28
z	0.60	0.59	**0.64**	0.46	0.60	0.41	0.72*	0.30
z h_c^{-1}	**-0.72***	**-0.73***	**-0.66**	**-0.48**	**-0.52**	**-0.39**	**-0.47**	**-0.35**
LAI h_c^{-1}	-0.56	-0.54	-0.53	*-0.07*	*-0.26*	*0.09*	*-0.13*	*0.01*
croplands, grasslands								
h_c	**0.54***	**0.59****	**0.34**	0.42	**0.61****	0.50*	**0.85****	-0.25
LAI	*0.01*	0.06	*-0.13*	**-0.49**	*-0.04*	**-0.33**	*0.03*	**-0.32**
z	0.04	*0.01*	-0.23	**0.64****	0.59**	**0.70****	0.48	*-0.03*
z h_c^{-1}	**-0.48**	**-0.66****	-0.47	*-0.16*	**-0.45**	*-0.20*	**-0.59****	0.12
LAI h_c^{-1}	-0.34	-0.47	**-0.47**	-0.36	-0.30	-0.31	-0.37	-0.06

Table A1: Count of half-hourly time steps during daylight (CoD) per considered time period for each study site, corresponding percent fractions of CoD of high-quality (HQ) and percent fractions of these HQ-time steps with a found partitioning solution for each method version. Bold (italic) lettering indicates the highest (lowest) fraction of solutions for each site. Plus (minus) indicates the highest (lowest) fraction for each method version.

method	site / time period	CoD	rel CoD used (HQ)	rel HQ with part-itioning solution	site / time period	CoD	rel CoD used (HQ)	rel HQ with part-itioning solution
SK10 WUE$_{meanT}$				84.4				26.2
SK10 WUE$_{MOST}$	**Forest_LO**		91.8	82.1	**Maize_DI_06**		84.8	34.5
SK10 WUE$_{OLR}$	08.-14.07.2003	231		65.6	14.-16.06.2007	99		*23.8* -
TH08 CV Q1, REA Q1				**99.4**				**98.4**
TH08 CV H, REA H			68.0	86.0			63.6	82.5
TH08 CV GMM				*59.2*				57.1
SK10 WUE$_{meanT}$				75.7				90.4
SK10 WUE$_{MOST}$	**Forest_HH**		89.2	76.2	**Maize_DI_07**		97.9	88.3
SK10 WUE$_{OLR}$	03.-09.07.2016	231		74.8	14.-16.07.2007	96		77.7
TH08 CV Q1, REA Q1				**100.0** +				**98.7**
TH08 CV H, REA H			59.7	55.8			78.1	*50.7*
TH08 CV GMM				*51.4*				52.0
SK10 WUE$_{meanT}$				80.6				95.3 +
SK10 WUE$_{MOST}$	**Forest_WU**		78.0	78.8	**Maize_DI_08**		94.5	94.2
SK10 WUE$_{OLR}$	18.-24.05.2015	218		70.6	04.-06.08.2007	91		89.5
TH08 CV Q1, REA Q1				**100.0** +				**100.0** +
TH08 CV H, REA H			55.5	74.4			80.2	*45.2*
TH08 CV GMM				*51.2*				57.5
SK10 WUE$_{meanT}$				88.3				57.3
SK10 WUE$_{MOST}$	**Forest_WA**		92.8	91.7	**SugarBeet_SE_06**		92.7	57.3
SK10 WUE$_{OLR}$	04.-10.07.2016	222		89.3	20.-22.06.2017	96		52.8
TH08 CV Q1, REA Q1				**100.0** +				**98.6**
TH08 CV H, REA H			75.2	65.9			76.0	58.9
TH08 CV GMM				*50.3*				*47.9*
SK10 WUE$_{meanT}$				*33.3*				72.9
SK10 WUE$_{MOST}$	**Forest_LA**		84.1	38.4	**SugarBeet_SE_08**		77.8	71.4
SK10 WUE$_{OLR}$	24.-30.09.2017	164		56.5	02.-04.08.2017	90		72.9
TH08 CV Q1, REA Q1				**100.0** +				**100.0** +
TH08 CV H, REA H			54.9	93.3 +			62.2	*37.5*
TH08 CV GMM				58.9				41.1
SK10 WUE$_{meanT}$				95.0				80.6
SK10 WUE$_{MOST}$	**Forest_MMP**		84.8	95.0 +	**SugarBeet_SE_09**		92.3	81.9
SK10 WUE$_{OLR}$	06.-12.06.2014	211		93.3 +	04.-06.09.2017	78		81.9
TH08 CV Q1, REA Q1				**100.0** +				**98.3**
TH08 CV H, REA H			73.0	70.8			76.9	25.0 -
TH08 CV GMM				*60.4*				*16.7* -
SK10 WUE$_{meanT}$				73.9				56.7
SK10 WUE$_{MOST}$	**Forest_SC**		87.4	75.2	**Wheat_SE**		93.8	52.2
SK10 WUE$_{OLR}$	01.-07.04.2017	175		77.1	03.-05.06.2015	96		46.7
TH08 CV Q1, REA Q1				**99.3**				**98.6**
TH08 CV H, REA H			77.7	47.1			77.1	*25.7*
TH08 CV GMM				*40.4*				32.4

(continued)

Table A1 continued:

method	site / time period	CoD	rel CoD used (HQ)	rel HQ with partitioning solution	site / time period	CoD	rel CoD used (HQ)	rel HQ with partitioning solution
SK10 WUE$_{meanT}$				*21.1* -				50.6
SK10 WUE$_{MOST}$	**Grass_RO**		91.7	*32.7* -	**Barley_SE**		82.3	51.9
SK10 WUE$_{OLR}$	15.-21.07.2013	217		28.6	27.-29.05.2016	96		58.2
TH08 CV Q1, REA Q1				**100.0** +				**98.5**
TH08 CV H, REA H			73.3	53.5			67.7	*26.2*
TH08 CV GMM				53.5				27.7
SK10 WUE$_{meanT}$				*31.3*				64.6
SK10 WUE$_{MOST}$	**Grass_WU**		82.1	38.0	**Intercrop_SE**		91.5	70.8
SK10 WUE$_{OLR}$	18.-24.05.2015	218		40.8	23.-25.09.2016	71		73.8
TH08 CV Q1, REA Q1				**100.0** +				**98.2** -
TH08 CV H, REA H			58.7	90.6			80.3	35.1
TH08 CV GMM				88.3 +				*28.1*
SK10 WUE$_{meanT}$				*34.8*				
SK10 WUE$_{MOST}$	**Grass_FE**		82.0	36.0				
SK10 WUE$_{OLR}$	11.-17.07.2015	217		39.9				
TH08 CV Q1, REA Q1				**100.0** +				
TH08 CV H, REA H			58.5	46.5				
TH08 CV GMM				65.4				